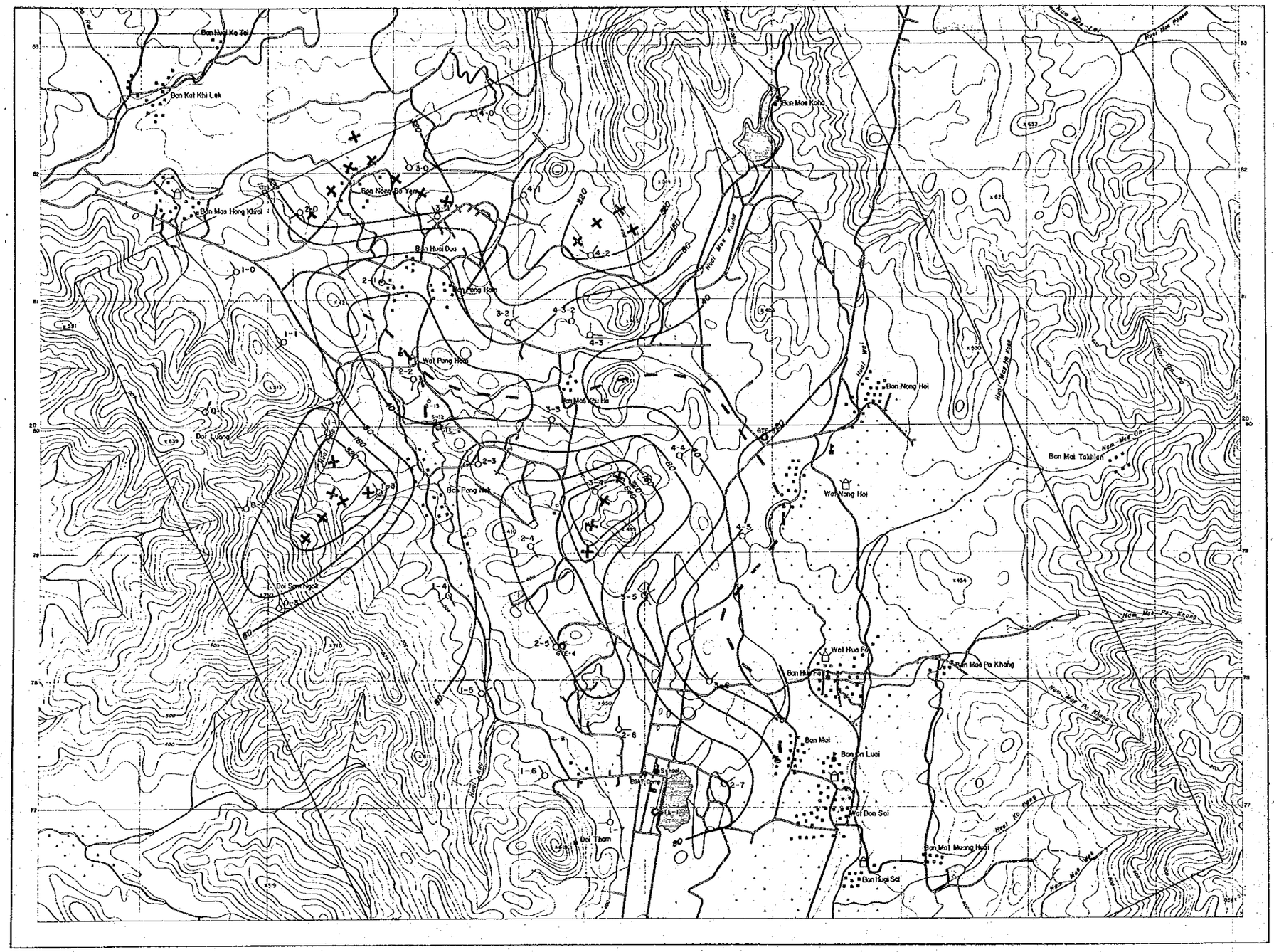

THE PRE-FEASIBILITY STUDY
ON
THE SAN KAMPAENG GEOTHERMAL DEVELOPMENT PROJECT
IN THE KINGDOM OF THAILAND

APPARENT RESISTIVITY ISOCONTOURS
(Period 1.1304sec)

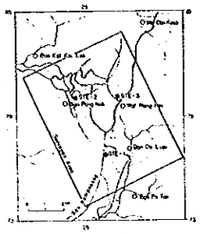

JAPAN INTERNATIONAL COOPERATION AGENCY
ELECTRICITY GENERATING AUTHORITY OF THAILAND
DEPARTMENT OF MINERAL RESOURCES
CHIANG MAI UNIVERSITY

0 500 1000m

LEGEND

- Confirmed road
- Unconfirmed road
- Stream
- Village
- Wat
- School
- Rice field
- Dam (water reservoir)
- 80 — Apparent resistivity contour (Ω-m)
- +++ High resistivity anomaly
- Low resistivity anomaly
- 3-5 — Measurement point

Fig. 1.5-5 Apparent Resistivity

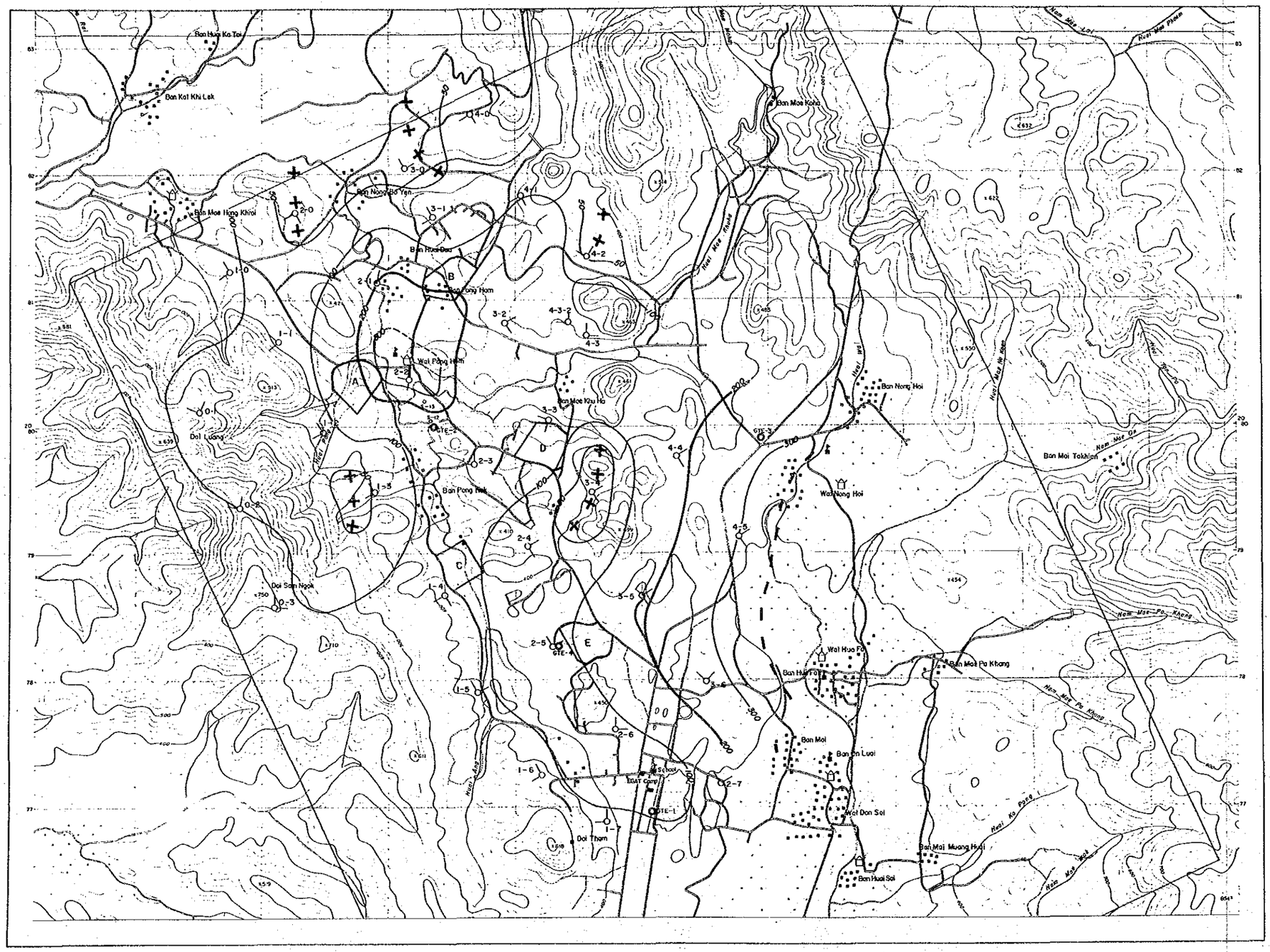

THE PRE-FEASIBILITY STUDY
ON
THE SAN KAMPHAENG GEOTHERMAL DEVELOPMENT PROJECT
IN THE KINGDOM OF THAILAND

TOTAL CONDUCTANCE

JAPAN INTERNATIONAL COOPERATION AGENCY
ELECTRICITY GENERATING AUTHORITY OF THAILAND
DEPARTMENT OF MINERAL RESOURCES
CHIANG MAI UNIVERSITY

LEGEND

- Confirmed road
- Unconfirmed road
- Stream
- Village
- Wat
- School
- Rice field
- Dam (water reserve)
- 300 — Total conductance (mhos)
- +++ Low conductance anomaly
- — — — High conductance anomaly
- 3-5 — Measurement point

Fig. 1.5-6 Total Conductance

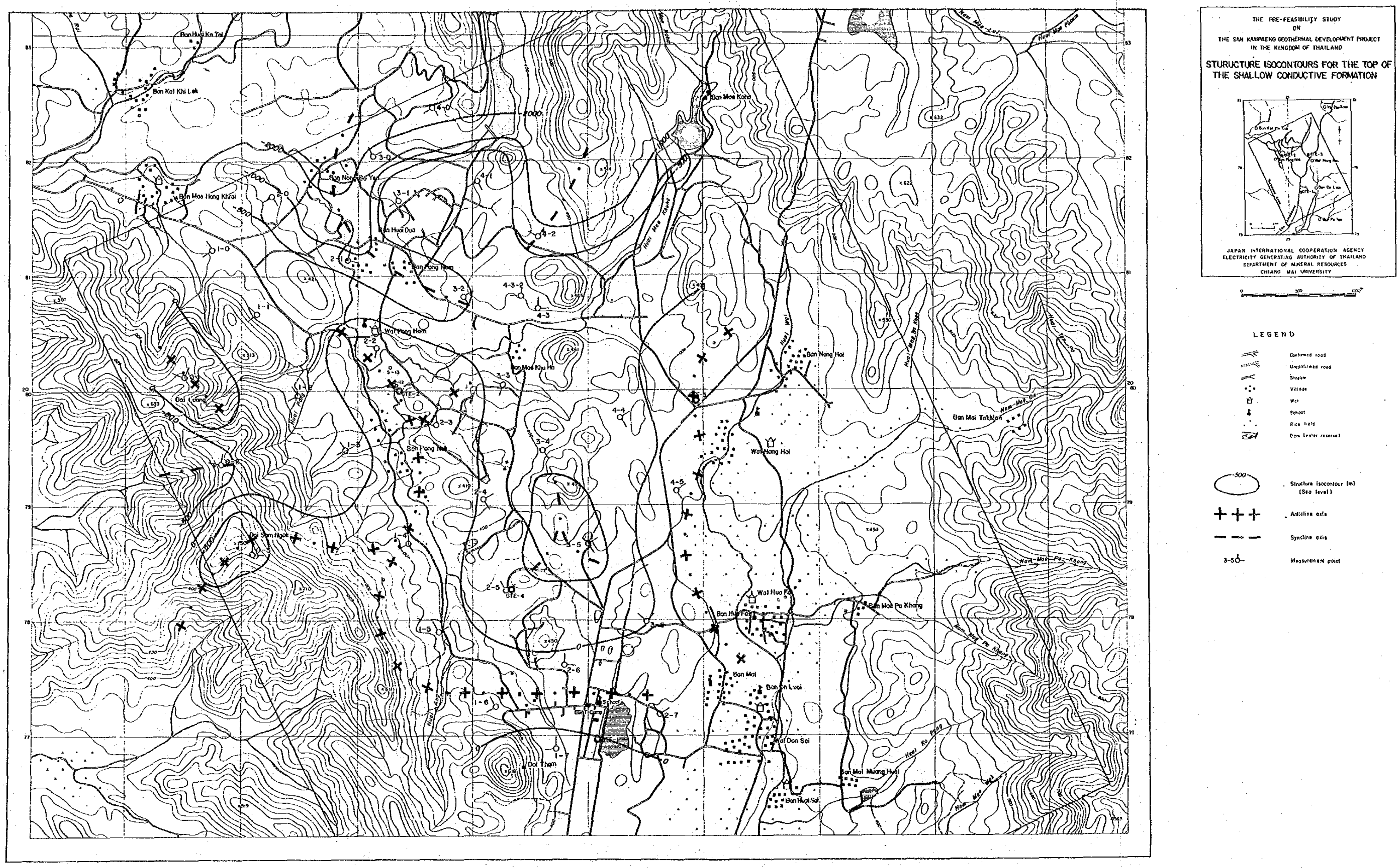

Fig. 1.5-7 Structure Isocontours for the Top of the Shallow Conductive Formation

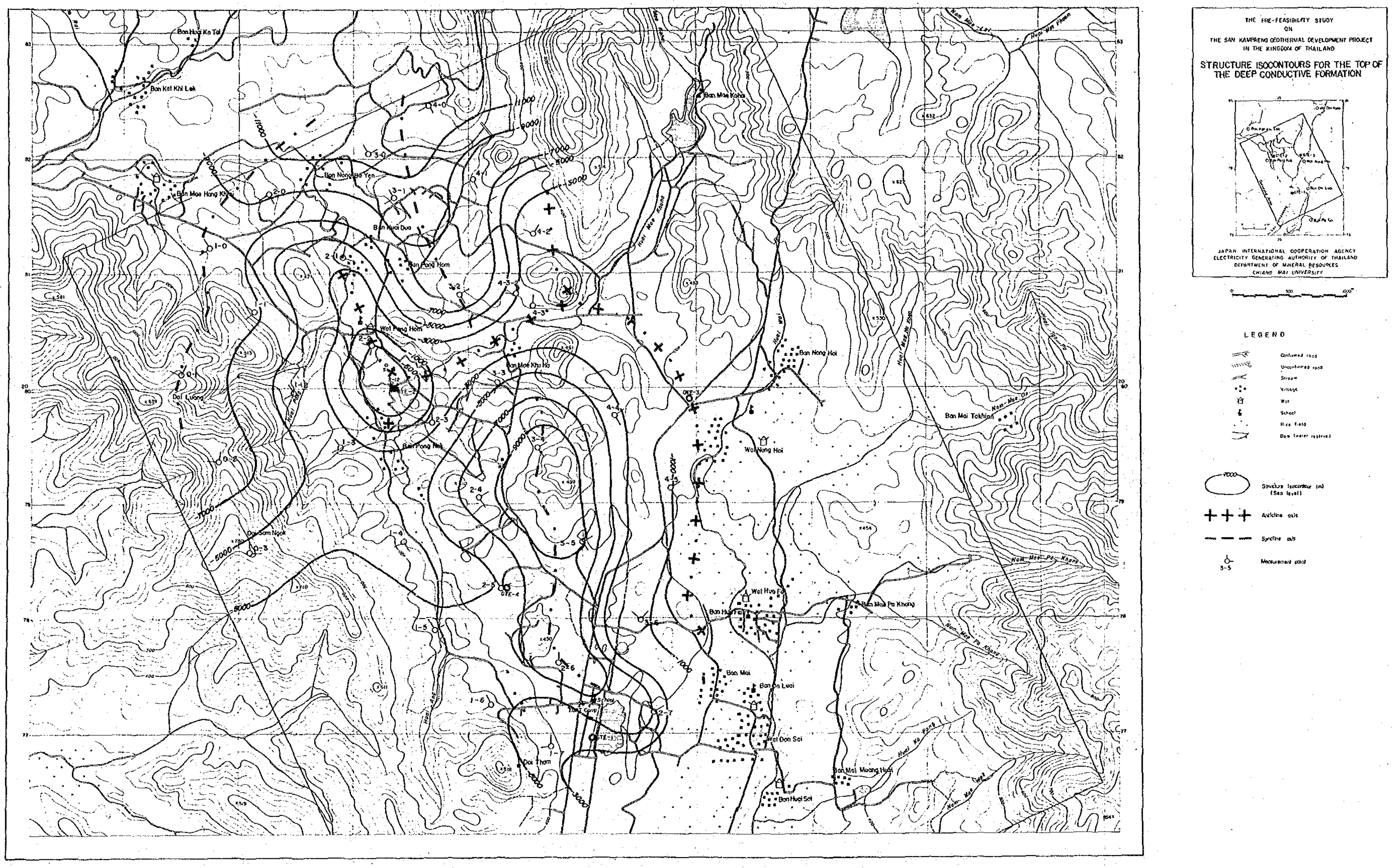

Fig. 1.5-8 Structure Isocontours for the Top of the Deep Conductive Formation

THE PRE-FEASIBILITY STUDY
ON
THE SAN KAMPHENG GEOTHERMAL DEVELOPMENT PROJECT
IN THE KINGDOM OF THAILAND

ISOPACHS OF THE OVERBURDEN OVERLYING THE DEEP CONDUCTIVE FORMATION

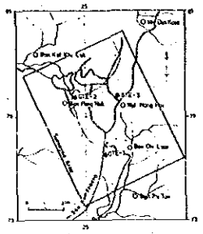

JAPAN INTERNATIONAL COOPERATION AGENCY
ELECTRICITY GENERATING AUTHORITY OF THAILAND
DEPARTMENT OF MINERAL RESOURCES
CHIANG MAI UNIVERSITY

0 500 1000

LEGEND

- Confirmed road
- Unconfirmed road
- Stream
- Village
- Wat
- School
- Rice field
- Dam (water reserve)
- 7000 — Isopach of the overburden (m)
- 3-5 — Measurement point

Fig. 1.5-9 Isopachs of the Overburdern Overlying the Deep Conductive Formation

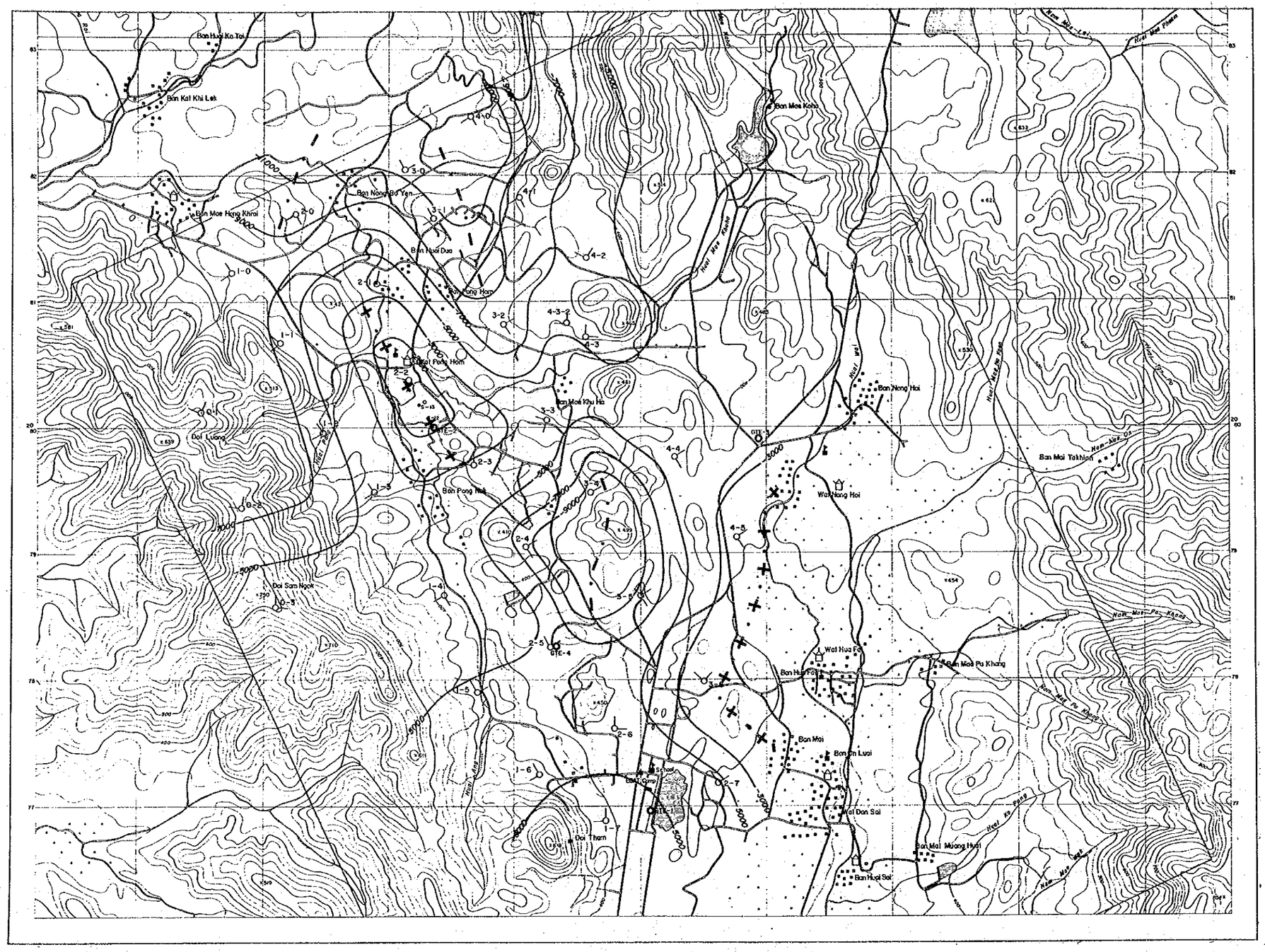

THE PRE-FEASIBILITY STUDY
ON
THE SAN KAMPAENG GEOTHERMAL DEVELOPMENT PROJECT
IN THE KINGDOM OF THAILAND

TOP OF ELECTRICAL BASEMENT

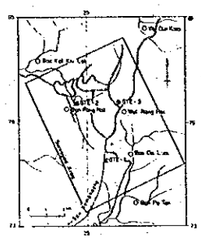

JAPAN INTERNATIONAL COOPERATION AGENCY
ELECTRICITY GENERATING AUTHORITY OF THAILAND
DEPARTMENT OF MINERAL RESOURCES
CHIANG MAI UNIVERSITY

0 500 1000m

LEGEND

- Confirmed road
- Unconfirmed road
- Stream
- Village
- Wat
- School
- Rice field
- Dam (water reserve)
- 9000 — Structure contour (m) (Sea level)
- +++ Anticline axis
- — — — Syncline axis
- 3-5 — Measurement point

Fig. 1.5-10 Top of Electrical Basement

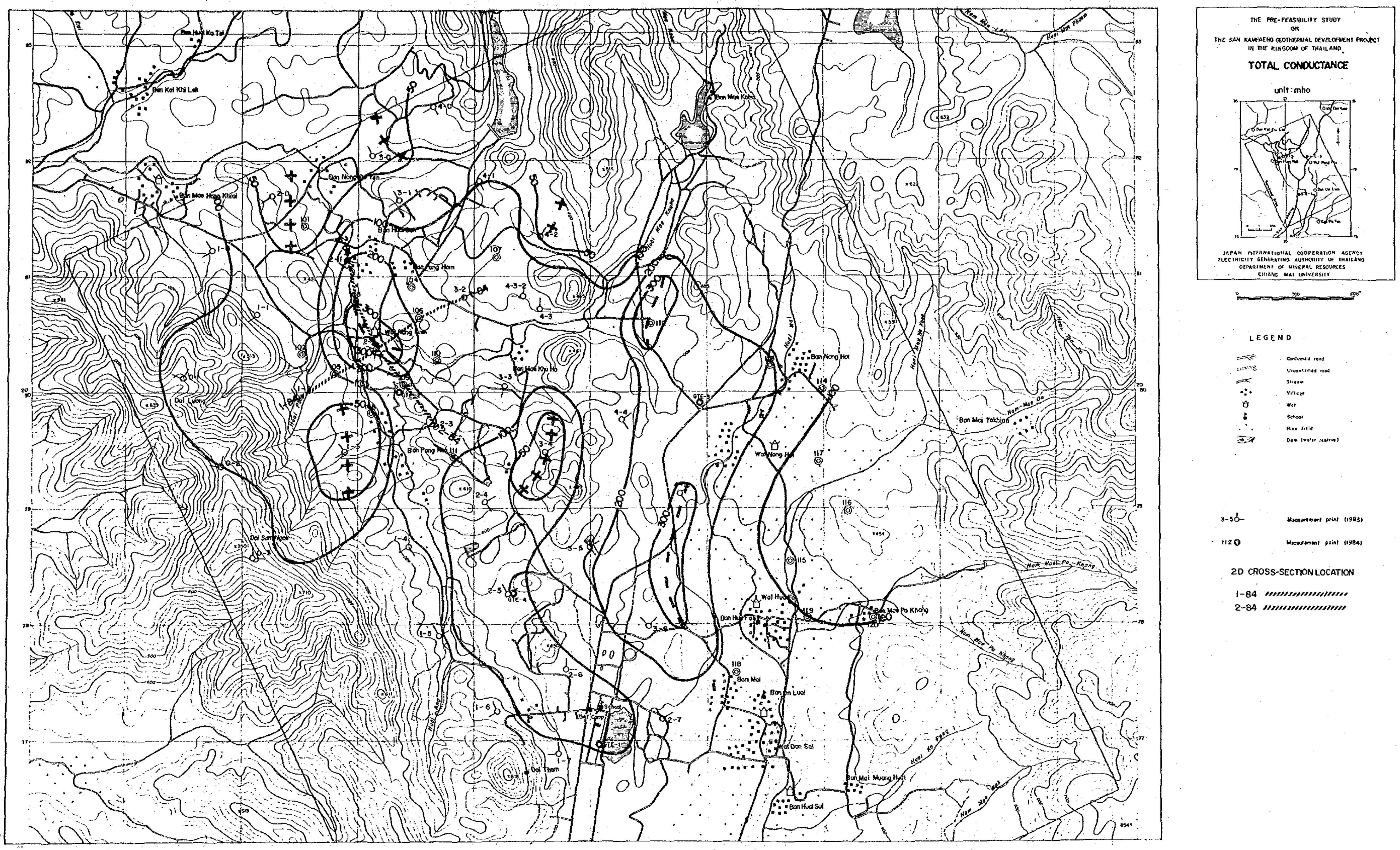

Fig. 1.5-11 Total Conductance

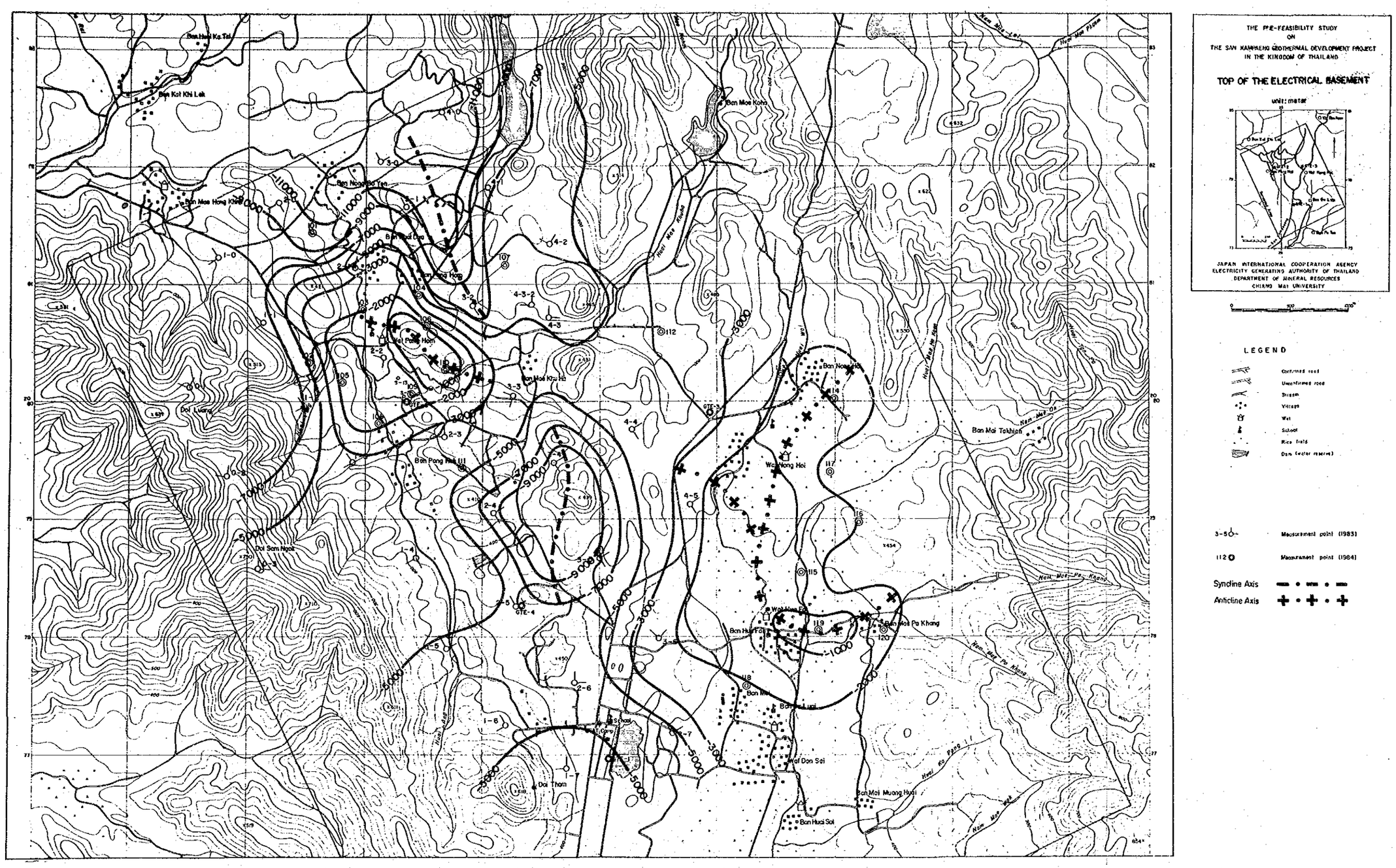

Fig. 1.5-12 Top of Electrical Basement

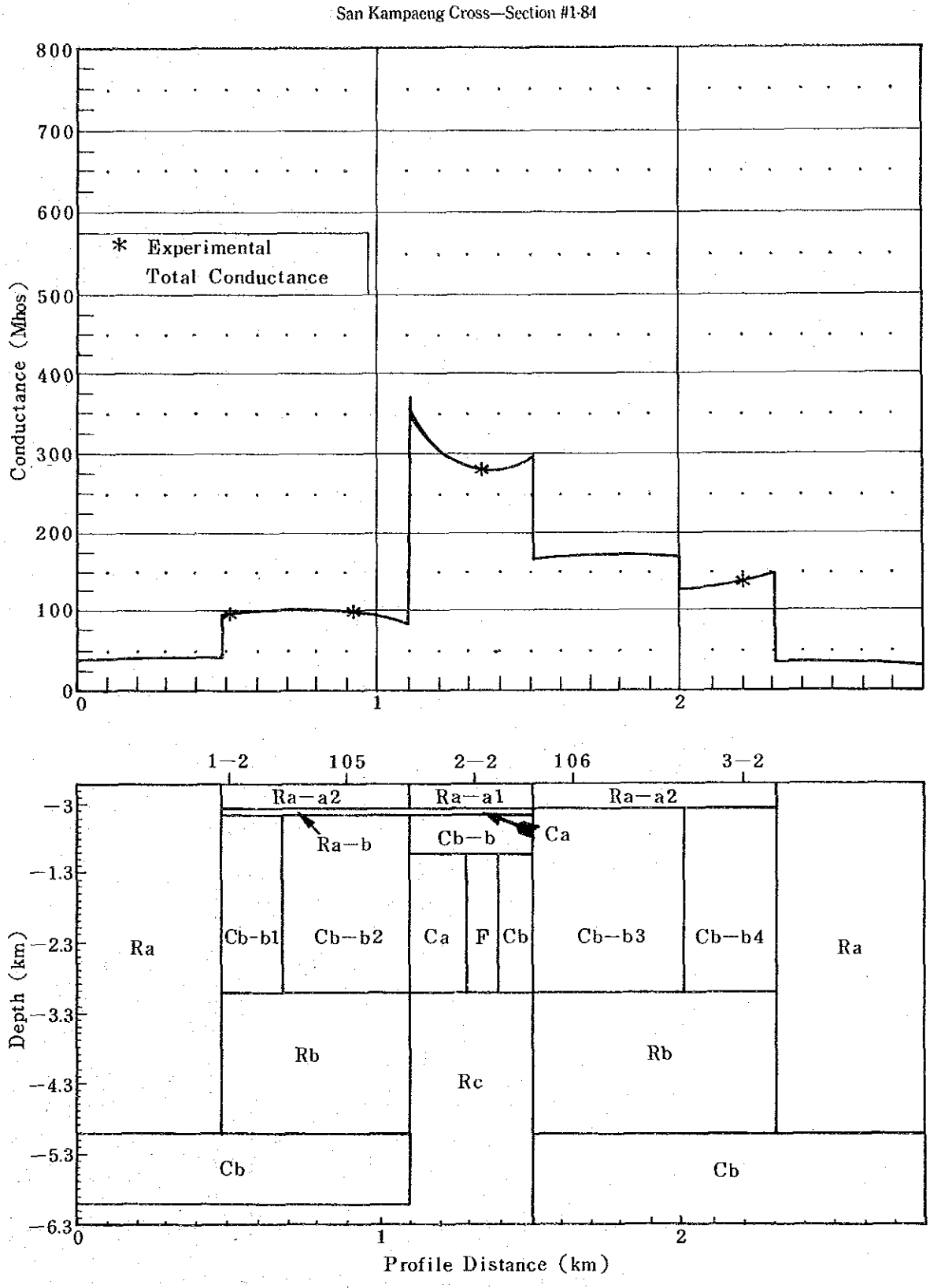

Fig. 1.5-13 Resistivity Profile (A)

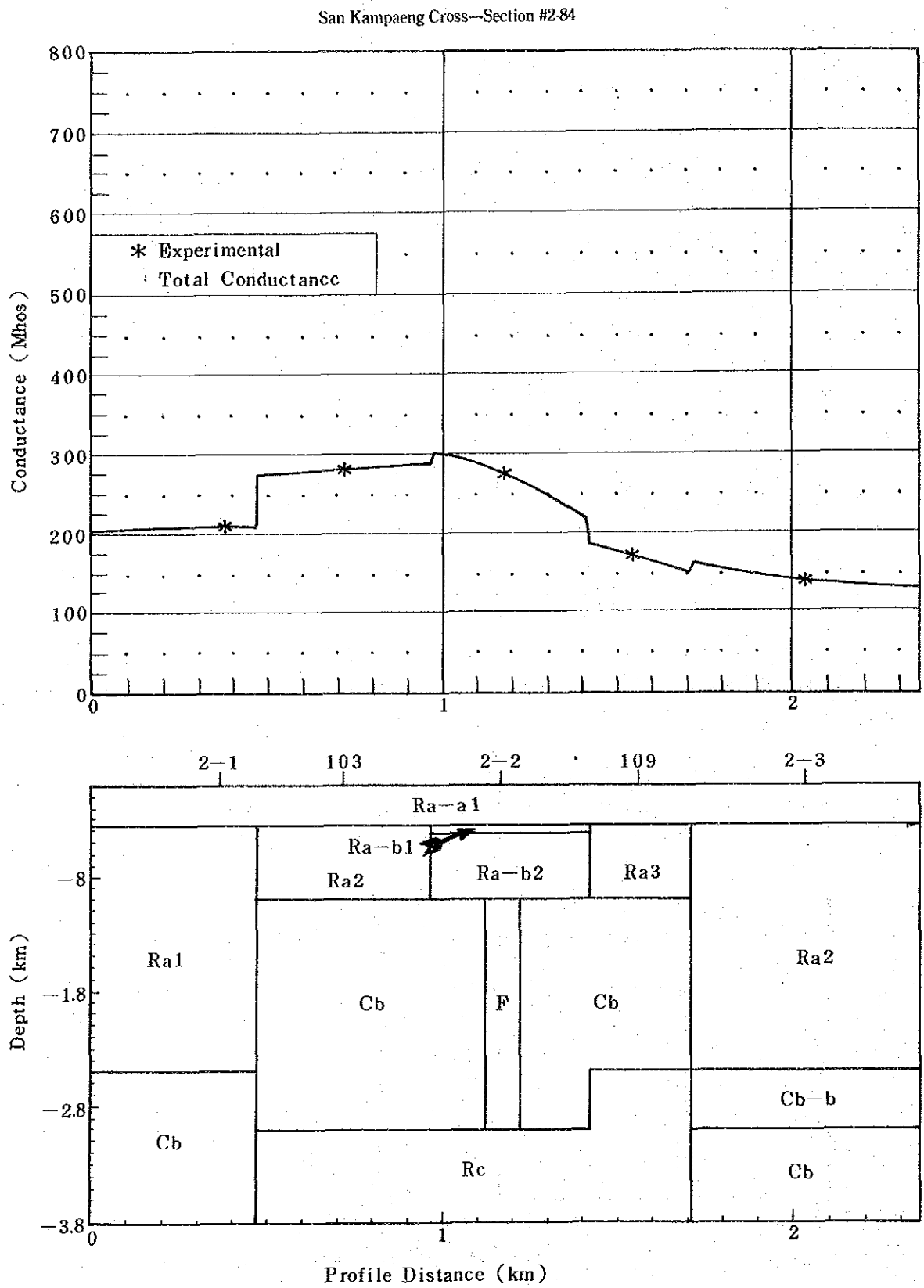

Fig. 1.5-14 Resistivity Profile (B)

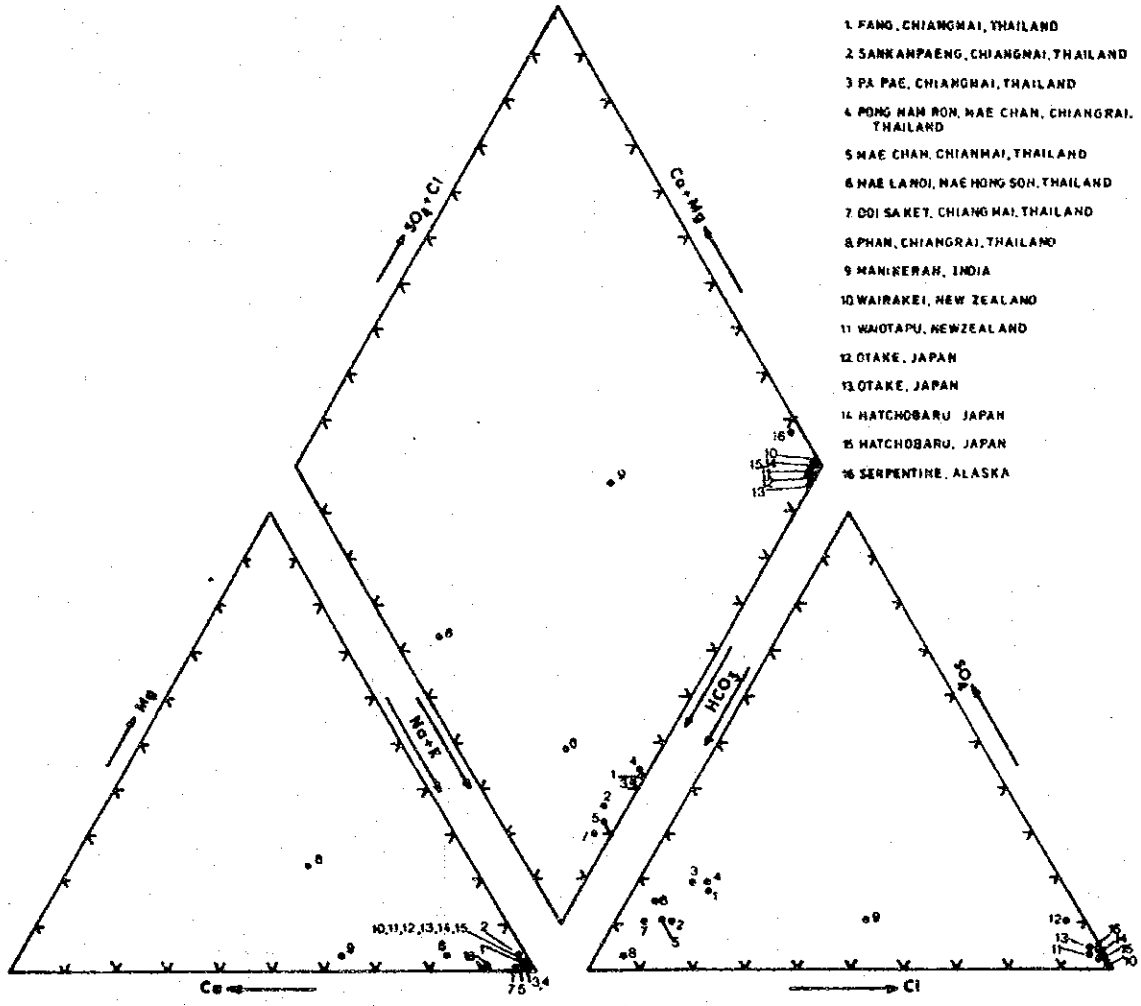

Fig. 1.6-1 Hydrochemical Characteristics of Thermal Waters from Northern Thailand and Other Parts of the World

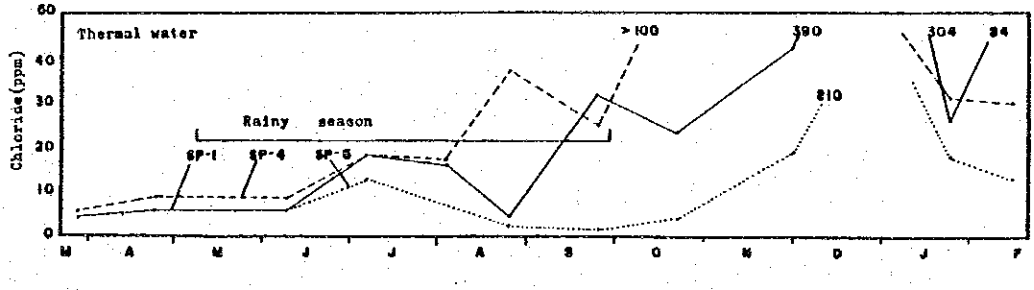

Fig. 1.6-2 Variation of Chloride Concentrations with Time in San Kampaeng Area

Table 1.1-2 Identification of Fossils

Sample Number	T - 099	E - 051	E - 055	W - 011	W - 015
Rock Name	Limestone	Limestone Breccia	Limestone	Limestone breccia	Limestone
Locality	X = 29,670 E Y = 77,280 N	X = 25,310 E Y = 76,940 N	X = 25,510 E Y = 77,630 N	X = 25,930 Y = 80 780	X = 25 720 E Y = 79,680 N
Age	Middle Permian	Carboniferous	No Determined	No Determined	Middle ? Permian
Fossils	Fusulinid Neoschwagerina Sumatrina Parafusulina ? Chusenella ? Crinoid Stem: Algae:	Fusulinid: Profusulinella ?? Coral flakes Bryozoa Algae ?	Crinoid Stem	Algae ?	Fusulinid: Schubertella Sp ? Kahlerina Crinoid stem Endothyrida Algae
Remark	Neoschwagerina and Sumatrina indicate that the strata is middle-Permian in age. Most of fusulinid are deformed and partly broken.	This strata is not exactly determined in age, because Fusulinids are rate and imperfect. They are asumed as Profusulinella of middle Carboniferous age for their size and shell structure. However, it is doubtful in age because an axial plane is not dtestable.	This rock is highly recrystallized. Geological age is impossible to determine because of only crinoid stems.	Rock facias is resemble to E-051 No age-determinable fossils are detected and no fossils in colitic limestone pebble are recognized.	Schubertella is found in early – middle Permian formation and Kahlerina is observed in middle Permian formation It shows most possibility that the strata is middle Permian in age.

Table 1.1-4 X-ray Diffraction Data of Altered Rocks (1)

No.	Constituent Mineral / Sample Number	Quartz	Calcite	Plagioclase	K-feldspar		Halloysite	Montmorillonite	Saponite	Sericite	Chlorite	Kaolinite	Alunite	Gypsum	Jarosite	Marcasite	Pyrite	Goethite	Gibbsite		Rutile	Anatase	Hornblende?	Stilpnomelane?
1	T-056	◎		◎	●			◎			△			●			△						△	
2	T-057	◎	△	◎	●			△			△			△			△						△	
3	T-058	◎		◎	●			◎			△			△			△						△	
4	T-059	◎		◎	●			◎			△			△			△						△	
5	T-060	◎		◎	●			◎			△			△			△						△	
6	T-061	◎		○	●			◎			△			△			○						△	
7	T-062	○		◎	●			◎			●			△	●		△						●	
8	T-063	△		◎	●			◎			△			△			○						△	
9	T-064	◎	◎	◎	●			◎			△			●			△						△	
10	T-065	◎		◎	●			◎			△			●			△						●	
11	T-066	○		◎	●			◎			○			●			○						△	
12	T-067	◎		◎	●			◎			△			●			△						△	
13	T-068	△		◎	●			△			△			△	●		◎						△	
14	T-069	◎		△				◎						△	△		△						●	
15	T-070	△	○	○	△			◎			○						○						△	
16	T-071	◎		◎				△		●	△			●			△						△	
17	T-072	◎		◎	●			△	●		△			●			△						△	
18	T-073	◎		◎	●			○	●		△			△			△						△	
19	T-074	◎		△	●			○	○		△			●			△						△	
20	T-075	●	◎	△				○	○		△			●			△						●	
21	T-076	◎		○	●			◎	◎		△			△			△						△	
22	T-077	◎								△		●												
23	T-078	◎		△				○		●		●		△	●		△						●	
24	T-079	◎		△				◎									○							
25	T-081	◎								△		△						●						
26	T-087	◎								○		△						●						
27	T-091	◎								○	△	○						●			●			
28	T-097	◎	●	◎	○						◎								○					○
29	T-104	◎								△		◎										●		
30	E-002	◎								△		△												
31	E-003	◎								△		△						△						
32	E-010	◎								○		○										△		
33	E-011	◎			◎					△		△												
34	E-014	◎								○		○										●		
35	W-004	◎								○		△												
36	W-021	△		○				○				△						△						
37	W-022	○		○				◎				△												
38	W-024	◎								○		◎						△						
39	W-025	◎								○		○						●				●		
40	W-026	◎								◎		○						△						

Table 1.1-4 X-ray Diffraction Data of Altered Rocks (2)

No.	Constituent Mineral / Sample Number	Quartz	Calcite	Plagioclase	K-feldspar		Halloysite	Montmorillonite	Saponite	Sericite	Chlorite	Kaolinite	Alunite	Gypsum	Jarosite	Marcasite	Pyrite	Goethite	Gibbsite		Rutile	Anatase	Hornblende?	Stilpnomelane?
41	W-027	◎								○		○										•		
42	W-028	◎										△						○				△		
43	W-029	◎								△		△						○						
44	W-030	◎								△		△						△				△		
45	W-031	◎					○			•								△				△		
46	W-032	◎					○											○				○		
47	W-033	◎					△			•								○				△		
48	W-034	◎					△			△								○				△		
49	W-035	◎					△			△								△				•		
50	W-036	◎					○			○								•				△		
51	T-003								◎														•	
52	T-004	•		◎					△		•		•				•							△
53	T-007	◎											◎								•			
54	T-009	◎		○				△		•		•					•						•	
55	T-010	◎		△	•					•		•		△									•	
56	T-011	◎		△				○		•		•		•			△							
57	T-012	◎		△				○		•		•		•			△							
58	T-013	◎		△				○		•	•			•			△						•	
59	T-014	◎		△				◎		•				•			△							
60	T-015	◎		○				△		•	•			•			○						•	
61	T-016	◎		○				△		•	•			•			△						•	
62	T-017	◎		△				△		•				•			△						•	
63	T-018	◎		○				△		•	•			•			○						•	
64	T-019	◎		△				△		•	•	•		△			△						•	
65	T-020	◎	○	△				△		•	•			△			△						•	
66	T-021	◎						△		•				△			•							
67	T-022	◎		△						•							△							
68	T-023	◎						△		•	•			•			△						•	
69	T-024	◎		△				△						•			•							
70	T-025	◎		△				△						•			△							
71	T-026	◎		△				△				•		•			△							
72	T-027	◎		△				△		•	•			△			△							
73	T-028	◎		△				△		•		•		△			△						•	
74	T-029	◎		△				○		•		•		•			•						•	
75	T-030	◎		△				○		•		•		△			△						•	
76	T-031	◎		△				△		•		•		△			△						•	
77	T-032	◎		△				△		•		•		△			△						•	
78	T-033	◎		△				△		•	•			△			△						•	
79	T-034	◎		○				◎			△			•			△						•	
80	T-035	○		◎	•			◎			•						△						•	

Table 1.1-4 X-ray Diffraction Data of Altered Rocks (3)

No.	Constituent Mineral / Sample Number	Quartz	Calcite	Plagioclase	K-feldspar	Pyroxene (Augite)	Biotite	Montmorillonite	Saponite	Sericite	Chlorite	Kaolinite	Alunite	Gypsum	Jarosite	Marcasite	Pyrite	Sphene	Gibbsite	Pumpellyite?	Rutile	Anatase	Hornblende?	Stilpnomelane?
81	T-036	◎		◎	●			◎			●			△			△						●	
82	T-037	◎		◎	●			○			●		●	△			△						●	
83	T-038	◎		◎	●			○						●		○	○						●	
84	T-039	◎		◎	●			○			●			△	△		△						△	
85	T-040	◎	◎	○	●			△			△			●			△						●	
86	T-041	○		◎	●			△			△			△			△						△	
87	T-042	◎		◎	●			◎			△			△	●		△						△	
88	T-043	◎		◎	●			◎			△			●			△						△	
89	T-044	◎		◎	●			△			●			●	△		○		△				△	
90	T-045	◎		◎	●			○			△			●			△						△	
91	T-046	◎	△	◎	●			△			△			△			△						△	
92	T-047	◎		◎	●			○			△			△			△						△	
93	T-048	◎	○	◎	●			○			△			△			△						△	
94	T-049	◎		◎	●			◎			△			●			△						△	
95	T-050	◎		◎	●			◎			●			△			△						△	
96	T-051	◎		○				◎							△									
97	T-052	◎		◎	●			△			△			△	●		○						△	
98	T-053	◎		◎	●			○			△			△			△						△	
99	T-054	△		◎	●			△			△			△			△						△	
100	T-055	◎		◎	●			◎			△						△							
101	T-001	●				◎					◎						●	△		△			●	
102	T-080	△		◎		○					△													
103	W-019	●		◎		○	●				△		●											

◎ Abundant
◎ Much
○ Common
△ Few
● Very rare

Table 1.2-2 Measurement Result of Rock Density (1)

Rock	No.	Weight in wet state		
		Weight in air (g)	Weight in water (g)	Density (g/cm^3)
Basalt	20	1469.9	971.9	2.95
〃	21	1769.9	1171.6	2.96
〃	22	417.4	279.2	3.02
〃	23	795.6	503.2	2.72
〃	24	1418.1	927.2	2.89
〃	25	723.4	472.2	2.88
〃	26	1072.5	715.7	3.01
〃	27	1280.4	839.0	2.90
〃	28	1645.6	1095.2	2.99
〃	29	873.6	573.4	2.91
〃	30	847.1	563.9	2.99
〃	81	1069.3	707.6	2.96
〃	82	1181.7	787.5	3.00
Tuff	1	1558.5	1003.8	2.81
〃	2	1201.9	770.9	2.79
〃	3	1092.6	702.8	2.80
〃	4	1109.1	734.4	2.96
Basaltic tuff	5	1268.0	829.6	2.89
Tuff	6	675.8	454.3	3.05
〃	7	1199.6	771.2	2.80
〃	8	1790.3	1202.7	3.05
〃	9	1997.1	1326.0	2.98
〃	10	1032.4	682.4	2.95
〃	11	840.4	562.6	3.03
〃		322.1	194.0	2.51
Tuff breccia	12	1033.7	679.2	2.92
〃	13	1020.3	667.5	2.89
〃	14	1204.0	781.2	2.85
〃	15	1493.6	979.8	2.91
〃	16	902.7	600.5	2.99
〃	17	1191.5	798.0	3.03
〃	18	1544.5	1028.1	2.99
〃	19	598.3	396.8	2.97
Limestone	52	394.5	250.0	2.73
〃	53	690.8	435.5	2.71
〃	54	1648.0	1034.9	2.69
〃	55	1783.2	1136.8	2.76
〃	56	741.1	465.1	2.69
〃	57	461.3	290.0	2.69
〃	58	524.5	330.0	2.70
Silicified limestone	83	1267.5	782.7	2.61
Limestone	59	1060.6	667.5	2.70
〃	60	1024.1	648.1	2.72
〃	61	1255.0	792.1	2.71
〃	62	498.5	319.8	2.79
〃	63	903.5	572.2	2.73
Chert	47	305.2	164.2	2.16
〃	48	1175.3	707.8	2.51
〃	49	1105.2	666.1	2.52
〃	50	998.6	598.3	2.49
〃	51	545.7	338.3	2.63

Table 1.2-2 Measurement Result of Rock Density (2)

Rock	No.	Weight in wet state		
		Weight in air (g)	Weight in water (g)	Density (g/cm^3)
Calcareous shale	31	451.6	281.6	2.66
Black shale	32	451.6	281.6	2.66
Shale	33	1373.7	807.9	2.43
Calcareous shale (fresh)	34	743.5	468.5	2.70
" (weathered)	35	1406.2	852.9	2.54
Shale	36	602.2	375.7	2.66
Black shale	79	736.1	455.1	2.62
Shale	84	672.9	385.5	2.34
"	37	691.8	438.0	2.73
"	38	1307.9	816.9	2.66
Weathered shale	39	388.4	190.3	1.96
Sandstone	40	696.0	427.7	2.59
"	41	641.8	396.3	2.61
"	42	655.2	394.6	2.51
"	64	528.5	321.0	2.55
"	65	237.3	145.6	2.59
"	66	367.5	226.5	2.61
"	67	1312.3	807.1	2.60
"	43	567.3	337.2	2.47
"	68	1436.7	886.6	2.61
"	78	1198.9	727.0	2.54
"		848.2	523.3	2.61
"	80	1094.5	659.6	2.52
"	44	1162.9	694.4	2.48
"	45	1265.3	777.2	2.59
"	46	1156.3	698.5	2.53
"	69	825.3	496.6	2.51
Granite	70	233.3	145.2	2.65
"	71	1574.5	954.5	2.54
"	72	1075.9	649.8	2.52
Quartz vein	73	696.0	427.7	2.59
"	74	1330.9	812.5	2.67
"	75	1024.0	629.7	2.60
"	76	968.0	592.0	2.57
"	77	1161.1	724.8	2.66

Table 1.3-3 Result of Susceptibility Measurment (1)

Rock	Resived No.	Apparent susceptibility (cgs/cc)	Correction coefficient		True susceptibility (cgs/cc)
Bosalt	20	6.2×10^{-6}	0.984	2.03	1.24×10^{-6}
〃	21	4.0×10^{-6}	0.984	1.97	7.75×10^{-6}
〃	22	4.3×10^{-6}	0.984	1.96	8.29×10^{-6}
〃	23	3.88×10^{-6}	0.984	1.85	7.06×10^{-6}
〃	24	2.8×10^{-6}	0.984	1.99	5.48×10^{-6}
〃	25	3.0×10^{-6}	0.984	1.93	5.70×10^{-6}
〃	26	4.1×10^{-6}	0.984	2.01	8.11×10^{-6}
〃	27	6.8×10^{-6}	0.984	1.99	1.33×10^{-6}
〃	28	1.62×10^{-6}	0.984	1.99	3.17×10^{-6}
〃	29	6.0×10^{-6}	0.984	1.98	1.17×10^{-6}
〃	30	5.8×10^{-6}	0.984	1.99	1.14×10^{-6}
〃	81	3.3×10^{-6}	0.984	2.00	6.49×10^{-6}
〃	82	1.21×10^{-6}	0.984	1.96	2.33×10^{-6}
Tuff	1	4.3×10^{-6}	0.984	1.87	7.91×10^{-6}
〃	2	5.1×10^{-6}	0.984	2.07	1.04×10^{-6}
〃	3	3.3×10^{-6}	0.984	1.88	6.10×10^{-6}
〃	4	3.6×10^{-6}	0.984	1.77	6.98×10^{-6}
Basaltic tuff	5	3.5×10^{-6}	0.984	2.06	7.09×10^{-6}
Tuff	6	6.0×10^{-6}	0.984	1.86	1.10×10^{-6}
〃	7	3.4×10^{-6}	0.984	2.00	6.69×10^{-6}
〃	8	3.7×10^{-6}	0.984	1.97	7.17×10^{-6}
〃	9	7.0×10^{-6}	0.984	2.00	1.38×10^{-6}
〃	10	3.9×10^{-6}	0.984	1.93	7.41×10^{-6}
〃	11	6.4×10^{-6}	0.984	1.98	1.25×10^{-6}
〃		1.3×10^{-6}	0.984	1.85	2.37×10^{-6}
Tuff breccia	12	8.75×10^{-6}	0.984	2.04	1.76×10^{-6}
〃	13	7.21×10^{-6}	0.984	1.88	1.33×10^{-6}
〃	14	2.5×10^{-6}	0.984	1.94	4.77×10^{-6}
〃	15	3.2×10^{-6}	0.984	1.99	6.27×10^{-6}
〃	16	7.0×10^{-6}	0.984	2.09	1.44×10^{-6}
〃	17	5.9×10^{-6}	0.984	1.92	1.11×10^{-6}
〃	18	6.1×10^{-6}	0.984	1.90	1.14×10^{-6}
Limestone	52	1.4×10^{-6}	0.984	2.48	3.42×10^{-6}
〃	53	1.3×10^{-6}	0.984	2.05	2.62×10^{-6}
〃	54	0.8×10^{-6}	0.984	1.94	1.53×10^{-6}
〃	55	0.9×10^{-6}	0.984	2.01	1.78×10^{-6}
〃	56	1.4×10^{-6}	0.984	1.96	2.70×10^{-6}
Limestone	57	2.1×10^{-6}	0.984	1.92	3.97×10^{-6}
〃	58	1.4×10^{-6}	0.984	1.99	2.74×10^{-6}
Silicified limestone	83	2.0×10^{-6}	0.984	1.95	3.84×10^{-6}
Limestone	59	4.3×10^{-6}	0.984	1.93	8.17×10^{-6}
〃	60	1.3×10^{-6}	0.984	1.97	2.52×10^{-6}
〃	61	1.2×10^{-6}	0.984	1.91	2.26×10^{-6}
〃	62	3.3×10^{-6}	0.984	2.10	6.82×10^{-6}
〃	63	1.9×10^{-6}	0.984	2.01	3.76×10^{-6}

Table 1.3-3 Result of Susceptibility Measurment (2)

Rock	Revised No.	Apparent susceptibility (cgs/cc)	Correction coefficient		True susceptibility (cgs/cc)
Chert (weathered)	47	1.2×10^{-6}	0.984	2.08	2.46×10^{-6}
〃	48	1.9×10^{-6}	0.984	1.95	3.65×10^{-6}
Chert	49	0.8×10^{-6}	0.984	1.83	1.44×10^{-6}
〃	50	1.4×10^{-6}	0.984	1.86	2.56×10^{-6}
〃	51	3.9×10^{-6}	0.984	1.88	7.21×10^{-6}
Calcareous shale	31	2.1×10^{-6}	0.984	1.91	2.63×10^{-6}
Black shale	32	1.4×10^{-6}	0.984	2.15	5.71×10^{-6}
Shale	33	4.6×10^{-6}	0.984	2.17	9.82×10^{-6}
Calcareous shale (fresh)	34	2.2×10^{-6}	0.984	1.90	4.11×10^{-6}
〃 (weathered)	35	4.3×10^{-6}	0.984	1.91	8.08×10^{-6}
Shale	36	7.1×10^{-6}	0.984	1.91	1.33×10^{-6}
Brocky shale	79	2.6×10^{-6}	0.984	1.88	4.81×10^{-6}
Shale	84	3.0×10^{-6}	0.984	2.07	6.11×10^{-6}
〃	37	3.6×10^{-6}	0.984	2.15	7.62×10^{-6}
〃	38	3.8×10^{-6}	0.984	1.93	7.22×10^{-6}
〃 (weathered)	39	0.6×10^{-6}	0.984	1.98	1.17×10^{-6}
Sand stone	40	3.0×10^{-6}	0.984	1.98	5.84×10^{-6}
〃	41	0.7×10^{-6}	0.984	1.93	1.33×10^{-6}
〃	42	1.6×10^{-6}	0.984	2.06	3.24×10^{-6}
〃	64	0.5×10^{-6}	0.984	1.93	9.50×10^{-6}
〃	65	0.9×10^{-6}	0.984	1.95	1.73×10^{-6}
〃	66	1.7×10^{-6}	0.984	2.04	3.41×10^{-6}
〃	67				
〃	43	1.1×10^{-6}	0.984	2.04	2.21×10^{-6}
〃	68	0.9×10^{-6}	0.984	1.99	1.76×10^{-6}
〃	78	0.7×10^{-6}	0.984	2.07	1.43×10^{-6}
〃		0.4×10^{-6}	0.984	1.92	7.56×10^{-6}
〃	80	0.6×10^{-6}	0.984	2.00	1.18×10^{-6}
〃	44	0.8×10^{-6}	0.984	2.12	1.67×10^{-6}
〃	45	4.1×10^{-6}	0.984	2.12	8.55×10^{-6}
〃	46	1.4×10^{-6}	0.984	2.01	2.77×10^{-6}
〃	69	1.2×10^{-6}	0.984	2.01	2.37×10^{-6}
Granite	70	1.5×10^{-6}	0.984	2.04	3.01×10^{-6}
〃	71	0.8×10^{-6}	0.984	1.95	1.53×10^{-6}
〃	72	0.8×10^{-6}	0.984	2.03	1.53×10^{-6}
Quartz vein	73	0.7×10^{-6}	0.984	1.85	2.40×10^{-6}
〃	74	0.2×10^{-6}	0.984	2.05	4.03×10^{-6}
〃	75	1.8×10^{-6}	0.984	1.93	3.42×10^{-6}
〃	76	0.3×10^{-6}	0.984	1.99	5.87×10^{-6}
〃	77	1.1×10	0.984	2.03	2.20×10^{-6}

2. Selection of Detailed Survey Area

The area for the detailed survey is delineated to estimate the possible geothermal reservoir in the San Kampang area based on the results of regional survey, i.e., geologic survey, gravity survey, etc.

In delineation, the surface geothermal manifestation as well as the results obtained from geologic structure analysis, deep electric survey and seismic survey are also taken into consideration.

2.1 Data on Surface Geothermal Manifestation

Geothermal manifestations include hot springs, fumaroles, heated ground, subsurface temperature taken at 10 m depth, hydrothermaly altered zones, distribution of gas concentation, etc. These geothermal showings seem to be the reflection of the geothermal reservoir at shallow depth.

Geothermal manifestations such as hot springs and famaroles are distributed in the southeast of Wat Pong Hom (about 0.5 km × 0.6 km) on the right bank of the main course the Huai Ang river.

Judging from the subsurface temperature at 10 m depth, measured by the counterparts of Thailand the high anomaly of ground temperature coincides with the distribution of these geothermal manlfestations, suggesting that the heat emanates from geothermal fluid.

The subsurface isothermal contour of 40°C at 10 m depth indicates an oval distribution with longitudinal axis in the NW-SE direction. The highest temperature is as high as about 103°C, observed in the S-13 exploratory well for the underground temperature survey. The isothermal area is distributed in almost a concentric circle centred on the S-13 well.

In this area the hydrothermal alteration zone is distributed around the geothermal manifestation. The alternation zoning sequence is, from the center to the outside: alunite zone - alollne zone - aloline. monmollionite zone - montmollionite zone - halloysite zone. It is considered that the zonal structure is formed by the flow of thermal water from the alunite zone (high temperature) to the halloysite zone (low temperature). It is highly possible that the temperature of the original thermal water which formed the hydrothermal alternation zone at the center of the alunite zone is higher than 200°C. However, it seems to be less than 200°C in almost to the area. In particular it is considered that the said temperature is must be lower than 100°C at the outer halloysite zone.

The distribution of the alteration zone roughly coincides with the geothermal manifestation; although there are some minor differences in distributions. The center of distribution of the subsurface temperature at 10 m depth (the center of the geothermal manifestation) is the S-13 well with a recorded temperature higher than 130°C. However, the alunlte belt which is considered as the center of the hydrothermal alternation zoning is located at a point about 30 m to the south of the GTE-2 exploratory well for the survey of subsurface temperature. The difference of the location of the geothermal manifestation area and the alunite zone suggests the migration with time of the center of geothermal field activity near the surface to the north.

The alteration zone is located, judging from the geologic structure, in the area between the

Huai Pong fault and the Ban Mae Khu Ha fault ,and it is estimated that the distribution of the alternation zone is structually controled by the branch-out fault of NW-SE trend passing through Ban Pong Nok.

The geochemical survey (CO_2, Hg, Rn) was conducted on the area including the San Kampaeng geothermal manifestation area. The distribution of these gases are considered to be the reflection of the intensity of activity of the geothermal manifestation.

From the result of CO_2 survey, it is elucidated that the high concentration anomaly for CO_2 coincides with the geothermal manifestation area, and the fault has a close relation with the CO concentration distribution.

From the study result of the surface manifestations, it is concluded that the goethermal reservoir at shallow depth in the San Kampaeng area is developed from the southeast of Wat Pong Hom to the southeast of Ban Pong Nok at the center course of the Huai Ang river.

2.2 Data on Geological Structure

The degree to which geological structure controls or bears a genetic relationship with, the geothermal manifestation discussed in section 2.1 was studied.

The study area is divided by both the Huai Pong fault and the Juai Mae Koen fault (both faults are nominal faults of NNW-SSE trend) into three areas, i.e., the Doi Luang uplifted zone (the western mountaneous area), the Ban Pong Hom subsided zone (the central lowland and the Mae Tha uplifted zone (the eastern hilly district). The geothermal manifestation area lies near the anticlinal axis at the western end of the Ban Pong Hom subsided zone and it is in the area surrounded by the Ban Hae Khu Ha fault of N-S direction, the Huai Pong fault and its branch-out fault in NW-SE direction. Therefore, it is estimated that a part of these faults may form the pathway for geothermal fluid from deep underground, and the sheared zone and similar structure at the wing of the anticlinal axis works as a geothermal reservoir. Based on the result of gravity survey, this area consists of three major areas, i.e. the eastern gravity high anomaly area, the central high gravity gradient anomaly zone and the western low gravity anomaly area. The thermal manifestations are within the western low gravity anomaly area and at the marginal zone of the low anomaly of tertiary residual gravity. The alteration and brecciation make the rock mass of low density, resulting in a low gravity anomaly area the limiting range of the geothermal reservoir.

Based on the result of magnetic survey, highly magnetic rock mass is distributed in the middle of the Kiu Lom Formation, and is found at the south of the Huai Wai fault, and along both the Huai Mae Khu Has and the Ban Mae Khu Ha fault. The distribution of the magnetic rock mass, therefore, indicates the intrusion of igneous rocks along the faults and suggests a structurally weak zone. However, it was difficult to detect the depth of the Curie point resulting from the geothermal activity, because the sedimentary rock near the geothermal manifestation area itself has very weak magnetism.

Finally, from the above mentioned examination of geological structure, it is highly possible that the distribution of a geothermal reservoir in the San Kampaeng area is located within the low gravity anomaly area, and the reservoir extends in the area surrounded by the Ban Mae Khu Ha fault, the Huai Pong fault and its branch-out fault in NW-SE direction.

2.3 Data on Results of Geophysical Surveys

Under this portion of the study, the results of MT Survey and seismic survey, which have great capability for eliciting vertical information, were examined to determine the extent of the deep geothermal reservoir.

The seismic survery revealed that geological structure in the survey area is divided into two areas, the west and the east, by a zone extending in nearly NS direction and connecting Ban Mae Khu Ha and Doi Tham. The west zone has upheaved and the east zone has subsided. The low frequency component is dominant in the west zone but is rare in the east. Because geothermal indications are in the low-frequency dominant area, the low-frequency dominant area is rich in fractures and has the capability of containing geothermal fluid.

The total conductance distribution and the apparent resistivity distribution of MT survey show fairly precisely the extent of a geothermal reservoir. Most of the survey area has total conductance below 200 mhos. High total conductance over 200 mhos is found around station 2-2, Wat Pong Hom, and the area between Wat Hong Hoi and Wat Hua Fai. The high conductance area is surrounded by an equi-conductance line of 200 mhos conforming to the contour of geothermal manifestation and is assumed to show the extent of the geothermal reservoir.

Two conductive layers, the one shallower than 500 m and the other between 1,000 m and 3,000 m, are found in the Wat Pong Hom area. The conductive layers are supposed to be geothermal reservoirs. The conductive layers extend in NW—SE direction and have width of 400 m to 500 m. The reservoir in the area is assumed to be of cylindrical shape and to extend vertically. A geothermal manifestation is assumed at the top of the reservoir.

As a result of examination of data from geothermal exploration survey, a geothermal reservoir in San Kampeng is judged to exist in the low gravity zone, surrounded by two N-S faults, the Huai Pong fault and Ban Mae Khu Ha fault, and their derivative NW-SE faults. The high conductance zone of the MT survey is considered to imply existence of a geothermal reservoir.

In this manner, the extent of the geothermal reservoir was assumed and the supplementary MT survey was carried out to pinpoint the location for an exploratory well in the detail survey area.

The results of the supplementary survey around Wat Pong Hom revealed that a high conductance zone (over 200 mhos) and a conductive zone (under 5 Ω-m) conform with the geological structure and underground temperature distribution. The conductive zone is assumed to be a fractured zone formed by two NNW-SSE faults, i.e., the Huai Pong fault and Ban Mae Khu He fault, and NW-SE faults. The fractured zone is assumed to be a geothermal reservoir in the area.

3. Drilling of GTE-7 and Results obtained

3.1 Selection of the Site

Fig. 3.1-1 shows the overlapped pattern of the distribution of faults, alteration types, subterranean temperature at the depth of 10 meters, and total conductance measured by the supplementary MT survey conducted in 1983 in the Ban Pong Nok District. The zones which are distributed in the geothermal manifestations and extending northwest to southeast in the figure coincide with areas exhibiting low resistivity under 5 ohm-m.

In the figure, the distribution of the high conductance zones showing over 200 mhos and the low resistivity zones showing under 5 ohm-m is concordant with the distribution of the subterranean temperature, and the low resistivity zones are coincident with sheared zones which were formed along the Huai Pong fault and the Ban Mae Khu Ha fault extending north-northwest to south-southeast, and the faults exdending northwest to southeast. Therefore it was judged that these sheared zones form geothermal reservoirs in the area.

Accordingly, the following model of the geothermal system in the area is proposed: geothermal fluid ascends along the sheared zones, after which it descends to the side of the sheared zones after reaching near the surface, forming a convection system. Fig. 3.1-2 shows the above mentioned model.

Fig. 3.1-2 shows the cross section extending east to west through the geothermal manifestations. However, judging from distribution of the subterranean temperature, geothermal reservoirs containing high temperature fluids, i.e. sheared zones, are asssmed to be further extended to the north of the known manifestations. That is the reason why the site for GTE-7 was selected to the north of the manifestations.

3.2 Drilling Work

3.2.1 Generalization

(1) Purpose of the drilling

The purpose of the drilling is to collect data on geological structure and subterranean temperature from the bore hole logging and inspection of cores. The drilling site to achieve the above mentioned purpose was selected based on the results of the first, second, and supplementary surveys.

(2) Outline of the drilling

1) Site: San Kampaeng Area, Thailand (Fig. 3.2-1)
2) Drill No. : GTE-7
   Inclination: Vertical
   Depth : 1,227.34 m
   Final bore hole size: HQ (101 mm)
3) Procedure: The drilling equipment was shipped by surface from Yokohama, Japan, to Bangkok, Thailand, in the middle of April 1984, and arrived in Bangkok in early May. It

was sent from Bangkok to San Kampaeng by EGAT, and set up at the site during the period from June 11 to July 15. The drilling was started on July 16, 1984.

The drilling was completed at the depth of 1,227.34 meters on February 26, 1985. In succession, measurement of the cores and bore hole logging were conducted. After finished all works, the JICA study team left the site on March 3, 1985, and arrived in Japan on March 8.

Fig. 3.2-2 and Tables 3.2-1 and 3.2-2 show the principal data on the drilling process and the works.

(3) Preparation and setting

About 6,400 m², 80 m × 80 m, of site had been prepared by EGAT for the drilling in advance, and storages for the equipment and a site office were set there.

Unpacking, inspection and arranging of the equipment arrived from Japan were started on June 11, 1984, and setting of the machine was finished on July 15.

3.2.2 Drilling Work

(1) Layout of the site

Fig. 3.2-3 shows the layout of the site.

(2) Equipment used

Tables 3.2-3 and 3.2-4 show the lists of the principal equipment used and consumed material for the work.

(3) Drilling work

Initially the drilling was planned to a depth of 1,500 meters. However it was stopped at the depth of 1,227.34 meters because of decrease of the drilling speed caused by hard rocks such as chert intercalated in hard sandstone and shale below a depth of 750 meters. Table 3.2-5 shows the outline of the process during the drilling work. The outline for each depth unit is as follows.

1) 0 to 4.20 meters

On July 16, 1984, the machine was test run and the hole was opened using a 14 inch casing pipe. After drilling up to 4.20 meters, a 14 inch SGP casing pipe was set and cemented to prevent collapse of the wall.

2) 4.20 to 30.00 meters

Twelve and a quarter inch toricone bits were used below the depth of 4.20 meters. Bed rock was encountered at the depth of 10.49 meters. HQ-WL coring was tried at a section between 13.14 and 16.78 meters, however it was abandoned because of unstable rock conditions. Non-core drilling was subsequently continued up to the depth of 30 meters. Specification of the tricorn bit drilling is as follows.

Mud Water	: Bentonite mud, speoific gravity 1.10, viscosity 26 - 30 sec/500cc
Bit	: Bit load 2 - 3 tons, rotation 50 rpm
Mud Pumping	: Volume ; 800 ~ 900 liters/min.

Pressure ; 10 kg/cm²

Mud Temperature : Entering ; 36.7 degrees in centigrade

Outflow ; 40.6 degrees in centigrade

After completion of drilling by toricone bits, 10 inch SGP casing pipes attached with float-shoe at the top were set at the hole, then fixed by cementing. The full hole cementing was conducted using 2,250 liters of cement slurry prepared at the specific gravity of 1.8, and overflow of the slurry was confirmed at the opening of the hole. After hardening of the cement, the remained cement in the tubes was drilled by 9 5/8 inch tricorn bit up to the depth of 30 meters. Then opening equipment such as B.O.P. was installed at the top of the 10 inch casing pipe.

Before starting HQ-WL coring at the depth of 30 meters, 4 1/2 inch provisional casing pipes were inserted into the hole to the depth of 30 meters to prevent hole deviation.

3) 30.00 to 200.00 meters

The hole was drilled by HQ-WL diamond bits. At the depth of 57.12 meters and 64.89 meters, squeeze cementing was conducted to prevent collapse of the wall because of unstable rock conditions. Weight of 1,440 kilograms of cement with the specific gravity of 1.8 was used the first time, and 1,320 kilograms of cement with the same specific gravity was used the second time.

Collapse of the wall occurred sometime during drilling, however, coring up to the depth of 200 meters was done by adjusting the specific gravity of the mud which consist of various rate of bentonite, libonite, and CMC. The mud was very effective for prevention of collapse and removing of cutting. The specific gravity of the mud ranges from 1.06 to 1.08, and the viscosity ranges from 25 to 30 sec/500cc.

The mud temperature shown in centigrade was as follows.

Depth (m)	50	100	150	200
Entering (°C)	40.3	44.3	45.9	48.1
Outflow (°C)	40.5	45.3	47.4	50.0

Nine and 5/8 inch toricone bits were used for reaming of the hole up to the depth of 200 meters. No special problem occurred in reaming this section. Specification of the reaming was as follows.

Bit : Bit load 2 ~ 3 tons, Rotation 50 rpm

Mud Pumping : Volume ; 80 ~ 900 ℓ/min.

Pressure ; 10 ~ 15 kg/m²

Bore hole temperature logging was performed at the hole after finishing reaming. The temperature at the bottom was 58.1 degrees centigrade. After logging, the hole was cleaned throughout, then 8 inch STPG-38-Sch40 casing pipes were inserted up to the depth of 199 meters, and they were fixed by cementing. The full hole cementing was done by two-plug method, and the overflow of the slurry was confirmed at the opening of the hole.

The volume, specific gravity, and mixing rate of the pressured cement slurry are as follows.

Volume : 4,180 liters
Supecific Gravity : 1.70
Mixing Rate : Geothermal cement 5,000 kg (S.G. 3.02), Retarder HR-4 17.5 kg (5,000 kg × 0.0035), Dispersion agents CFR-2 17.5 kg (5,000 kg × 0.0035)

Cement slurry was supplemented at the annular parts in the sizes of 10 inches and 8 inches. After hardening of the slurry, remaining cement in the tubes was drilled, then an inner tube pressure test at the point of float shoe and a outer tube pressure test at the cutting surface were conducted. The results of those are as follows.

Inner tube pressure test
Initially applied pressure : 30 kg/cm^2
Pressure after 20 min : 26 kg/cm^2
Outer tube pressure test
Initially applied pressure : 30 kg/cm^2
Pressure after 20 min : 5 kg/cm^2

Accordingly it was judged that the shield by the cement at the bottom of the tube was not enough. Subsequently, pressured cementing was conducted at the bottom of the tube. Specification of the cementing is as follows.

Cement slurry: 722 liters, specific gravity 1.8
Pressure: Initially applied: 30 kg/cm^2; after 20 min: 20 kg/cm^2

After drilling the cement, an outer tube test was conducted to confirm whether anomaly existed there or not. The result is as follows.

Pressure: Initially applied; 26 kg/cm^2
after 20 min ; 16 kg/cm^2

4) 200.00 to 504.00 meters

Rocks in the hole at the depth of 200 meters are alternation of shale and calcite intercalated by sandstone beds. Sheared zones exist throughout the section; therefore cores were frequently stuck in the tubes during the drilling. However, the inner hole conditions were generally good, and no trouble such as collapse of the walls and lost circulation were encountered. Specification of the drilling using HQ-WL diamond bits up to the depth of 504 meters is as follows.

Mud Water : Bentonite, Libonite, CMC, Asbestos
Specific Gravity; 1.05 - 1.10
Viscosity; 24 - 30 sec/500cc
Bit : Bit load; 0.5 - 1.5 tons

Rotation; 100 - 200 rpm
Mud Pumping : Volume; 100 - 150 liters/min.
Pressure; 15 - 18 kg/cm²

The mud temperature shown in centigrade is as follows.

Depth (m)	250	300	350	400	450	500
Entering (°C)	46.7	37.1	36.4	35.8	37.2	37.3
Outflow (°C)	51.8	41.0	44.0	44.0	45.0	43.6

The temperature in the bore hole at various depths shown in centigrade is as follows.

Depth (m)	210	250	277	299	330	358	389	420	450	480
Av.Temp (°C)	51.0	52.3	47.0	48.3	50.0	52.7	55.3	57.7	61.0	65.3

Reaming under the depth of 200 meters was done using 7 5/8 inch tricorn bits. No trouble was encountered in the work as well as in the case of HQ-WL drilling. Specification of the reaming is as follows.

Bit : Bid load ; 1.0 - 4.0 tons
Rotation ; 40 - 45 rpm
Mud Pumping : Volume ; 600 - 700 liters/min.
Pressure ; 10 - 20 kg/cm²

Bore hole logging at the depth of 500 meters was done by the EGAT logging team. Immediately after finished the logging, 6 inch STPG-38-Sch40 casing pipes were inserted. The pipes were attached with float collars and shoes, and special centralizers every 30 meters along the tubes to set the pipes in the center of the hole. Then full hole cementing using the two-plug method was conducted in the hole. Overflow slurry was confirmed at the opening of the hole. The volume, specific gravity, and mixing rate of the pressure cement slurry are as follows.

Volume : 7,124 liters
Specific Gravity : 1.8
Mixing Gate : Geothermal cement; 8,520 kg
Bentonite; 75.0 kg (8,520 kg × 0.0088)
Dispersion agents; CFR-2 29.8 kg (8,520 × 0.0035)
Note : FR-4 was not used because of low inner hole temperature.

Parts where sinking occurred after hardening of the cement were supplemented by additional slurry. After hardening of the cement, a pressure test of the inner and outer tubes was conducted, and no anomaly was found.

Inner tube pressure test

Initially applied pressure: 39.5 kg/cm²

Pressure after 10 min: 39 kg/cm²

Outer tube pressure test

Initially applied pressure: 46.0 kg/cm²

Pressure after 10 min: 45 kg/cm²

5) 504.00 to 1,002.75 meters

Rocks below the depth of 504 meters are shale, limestone, and sandstone, but chert is contained below the depth of 750 meters. Therefore the drilling speed by HQ-WL diamond bits became very slow, and the drilling schedule was very delayed compared with the initial one.

Mud water used for the drilling in this section was mainly composed of Telnite BH. Specification of the drilling is as follows.

Mud : Bentonite, Telnite BH, Asbestos, Telflow
Specific gravity; 1.05 - 1.10
Viscosity; 25 - 30 sec/500cc

Bid : Bit load; 1.0 - 1.5 tons
Rotation; 100 - 150 rpm

Mud Pumping : Volume; 100 - 130 liters/min.
Pressure; 10 - 15 kg/cm²

The mud temperature shown in centigrade is as follows.

Depth (m)	550	600	650	700	750	800	850	900	1,000
Entering (°C)	34.6	32.8	24.0	37.0	35.1	34.0	34.2	34.6	35.2
Outflow (°C)	43.8	43.7	42.2	41.8	42.9	41.1	42.2	46.9	42.3

The temperature in the bore hole at various depths shown in centigrade is as follows.

Depth (m)	510	540	570	600	630	661	689	720	749
Av.Temp (°C)	62.0	58.3	61.3	65.3	69.3	69.3	70.7	72.0	79.7

Depth (m)	810	840	870	900	930	960	990
Av.Temp (°C)	81.7	82.3	85.0	83.7	84.7	85.3	87.3

Reaming under the depth of 504 meters was done using 5 5/8 inch tricorn bits. In spite of very hard rocks there, the reaming speed was sufficient was scheduled. Reamed distance per single MH type tricorn bit was 51.4 meters, and that for the V3F type was 73.0 meters. Specification of the drilling is a follows.

Bit : Bit load; 1.0 - 3.0 tons
Rotation; 10 - 50 rpm

Mud Pumping : Volume; 350 liters/min.
Pressure; 15 - 20 kg/cm²

Bore hole logging was conducted under the instruction of Japanese engineers. After finishing logging, the hole was entirely cleaned. Then 4 1/2 inch SPO casing pipes were inserted. The casing pipes were attached with float collars and shoes, and fixed by a bellmouth attached about 2 meters below the opening of the hole. After that, full hole cementing using the two-plug method was performed. The volume, specific gravity, and mixing rate of the pressured cement slurry are as follows.

Volume : 12,040 liters
Specific Gravity : 1.8
Mixing Rate : Geothermal Cement; 14,400 kg
Bentonite; 126.7 kg (14,400 kg × 0.0088)
Dispersion agents; CFR-2 50.4 kg
(14,400 kg × 0.0035)
Note : HR-4 was not used because of low inner bore hole temperature.

After hardening of the cement, an inner and outer tube pressure test was conducted. The pressure measured is as follows.

Inner tube pressure test
Initially applied pressure: 32 kg/cm^2
Pressure after 20 min: no change
Outer tube pressure test
Initially applied pressure: 30 kg/cm^2
Pressure after 20 min: no change

Consequently it is judged that effect of the full hole cementing was very good.

6) 1,002.75 to 1,227.34 meters

During the drilling under the depth of 1,002.75 meters using HQ-WL diamond bits, a lost circulation problem was encountered at the depth of 1,005 meters. Telstop, Telseal and super asbestos were mixed in the mud to prevent lost circulation. After this procedure, 20 to 30 liters of mud water from a total inpouring 100 to 130 liters was lost per minute. However, no water level lowering occurred when the pump was stopped. Therefore the drilling was continued with the same mud water without any special countermeasure. Rocks in the hole are siliceous sandstones, and hardness of the rocks increased with depth. Accordingly, the drilling speed significantly decreased with depth. Consequently it was not possible to complete the initially planned 1,500 meters drilling within the scheduled term. The drilling was accordingly stopped at the depth of 1,227.30 meters. The temperature measured at the bottom of the hole was 101.2 degree centigrade. Specification of the drilling is as follows.

Mud Water : Bentonite, Telnite BH, Asbestos, Mud oil
Specific gravity; 1.02 - 1.05
Viscosity; 18 - 20 sec/500cc
Bit : Bit load; 1.5 - 2.0 tons
Rotation; 100 - 120 rpm

Mud Pumping : Volume; 100 - 130 liters/min.
Pressure; 15 - 20 kg/cm^2

The mud temperature shown in centigrade is as follows.

Depth (m)	1,050	1,100	1,150	1,200	1,227
Entering (°C)	35.5	34.5	37.1	33.1	33.2
Outflow (°C)	40.8	38.4	39.5	39.2	36.3

The temperature in the bore hole at various depths shown in centigrade is as follows.

Depth (m)	1,020	1,050	1,080	1,110	1,140	1,170	1,200	1,227
Av. Temp (°C)	87.0	94.0	96.3	96.7	98.3	97.3	99.8	101.2

(4) Mud Water for Drilling

The mud water was mixed according to the geology, drilling method (reaming or coring), temperature, of the hole, and was newly supplemented or exchanged when sharp change occurred in the foregoing conditions. The composition of the mud in each section of depth is as follows.

1) 0.00 to 30.00 meters

Mud mainly composed of bentonite was used for the drilling of the overburden and fragile rocks.

2) 30.00 to 200.00 meters

Bentonite mud was initially used of this section; however, it was gradually changed to libonite mud for maintenance of fluidity of the mud. Little lost circulation or temperature rise occurred. The specific gravity of the mud for reaming was raised only slightly without any change of basic composition, since the inner bore hole conditions were the same as for HQ-WL drilling.

3) 200.00 to 500.00 meters

Mainly libonite mud was used for this section since the inner bore hole temperature during HQ-WL core drilling did not change. The mud for reaming by 9 5/8 inch tricorn bit was also the same; however, telflow as a dispersion agent was added to the mud when reaming in mudstone since the specific gravity and viscosity of the mud increased. A mud water cooling tower was used for drilling below a depth of 200 meters.

4) 500.00 to 1,000.00 meters

Mud mainly composed of Telnite BH was used for the HQ-WL core drilling in this section. Telflow as a dispersion agent was added to the mud to prevent gelatinization, and water was added to lower the specific gravity and viscosity.

5) 1,000.00 to 1,227.30 meters

A small amount of Telnite BH mud was used for the HQ-WL core drilling after fixing 4 inch casing pipes; however, almost pure water was used for the main part of the drilling. At the depth of 1,005 meters, a lost circulation problem was encountered. Telstop(P), Telseal and other organic material were accordingly added to the mud to prevent such trouble. A little lost circulation was encountered during the drilling below the depth of 1,010 meters. However,

drilling was continued under unchanged conditions as no water table lowering occurred. Sometimes mud oil was added to the mud to maintain smooth rotation of rods.

(5) Cementing

Table 3.2-6 shows status of casing pipe cementing and maintenance cementing.

(6) Measurement of mud water temperature

Temperature of mud water at entering and outflow from the holes was measured and recorded every one hour, and referred to in assessing changes of inner hole conditions.

Table 3.2-7 and Fig. 3.2-4 show the results of measurements.

(7) Measurement of bottom hole temperature

Bottom hole temperature was measured by thermometers every 30 m. Thermometers were kept for 10 minutes at the hole bottom, then record for reading.

Table 3.2-8 shows the results of measurements.

(8) State of lost circulation during drilling

15.00 meters	: Volume;	80 liters/min.
	Countermeasure;	mixed Telstop P(75 kg)
	Effect;	lost circulation stopped.
455.00 meters	: Volume;	30 liters/min.
	Countermeasure;	mixed Telseal (20 kg)
	Effect;	lost circulation stopped
1,005.00 meters	: Water table;	0 meter
	Volume;	5 - 30 liters/min.
	Countermeasure;	applied 5,000 ℓ of dense mud water (mixed 90 kg of Telseal) to 1,062 m depth
	Effect;	Lost circulation continued unchanged.
		Lost circulation drilling performed.

(9) Status of setting of casing pipes

Fig. 3.2-5 shows the casing program.

(10) Record of bits used

Table 3.2-9 shows the record of toricone bits used for the drilling.

(11) Penetration rate and core recovery

Fig. 3.2-6 shows the penetration rate and the core recovery rate.

(12) Dismantlement

The dismantlement was conducted by the EGAT team under the instruotion of two JICA Japanese engineers during the period from August 29 to September 17, 1985. The equipment

dismantled was collected near the base camp, inspected and necessary maintenance performed.

3.3 Core Geology

3.3.1 Generalization

Following completion of the geothermal test well GTE-7 (1,227.34m deep) drilled cores were geologically studied. At the time of study, geology and alteration of core and factured zone were carefully studied to prepare a geologic column. Typical rock samples were taken every 30 meters for microscopic study, X-ray diffraction analysis and measurements on physical characteristics. Additional samples were taken for X-ray diffraotion analysis where argililzation was observed. Also, additional samples of quartz and/or calcite vein were taken to study filling temperature measurement by liquid content. The results of study are shown on the geological column (Fig.3.3-1~5). Furthermore, 500 m deep teet wells, GTE-2, GTE-4, GTE-5, GTE-6 all drilled by Thailand counterparts, along with four (4) surface locations were also studied for alteration. Samples for X-ray diffraction analysis and filling temperature measurement by liquid inclusion were taken. Sampling location and studied items are listed in the attached table of samples.

3.3.2 Geology

(1) 0 m to 58.2 m: Geology of this section is alternation of grey white sandstone and black shale. Sandstone is fine to medium grained arkosic sandstone with occasional fragments of black shale. This sandstone is banded in thickness of around 60 cm to less than 20 cm. Shale is black colored with carbonaceous matter and occurs as thin layers in the sandstone. The thickness of the layer reaches 20 cm in some places. Stratification shows moderate to steep dipping of more than 50°. In this section, 0 m to 13.14 m was soil. Non-oore drilling was done upto 30 m, but yielded cuttings suggest the same rock type as mentioned above. Fractured zonc was observed between 55.0 m to 56.0 m. Weak weathering is observed at shallower than 55 m, producing rather soft ground.

(2) 158.20 m to 181.50 m: Mainly composes of limestone including alternation of siltstone and shale between 160.00 to 163.80 m. Limestone is grey black colored and compact. Alternation is formed by pale green siltstone and carbonaceous black shale. Argillization and/or quartz veins are recognized at the boundary between limestone and the alternation. Strata dip is 40°~80°.

(3) 181.50 m to 274.40 m: Mainly composed of shale. Pale green to pale red mudstone and siltstone were observed between 181.50 m to 190.90 m. Alternation of black shale and dark grey chert was found between 237.40 m to 274.50 m. In the chert beds, core-recovery ratio decrease and fracturing is common. Dip of the formation is as steep as 85°.

(4) 274.40 m to 334.20 m: Composed of alternation of limestone and black shale. Limestone is black to grey black colored compact rock with intercalating layer of carbonaceous black colored shale. Both rock types are thiokly banded from several meters to around fifteen (15)

meters and dip 60°~80°.

(5) 334.20 m to 688.00 m: Mainly composed of black shale with intercalating layers of grey white colored medium grained sandstone. The section of 404.00 m to 434.00 m is characterized by thin (<1 m) layers of grey white to light grey colored chert, while between 54.20 m and 581.00 m grey colored limestone and chert (both thickness less than several meters) are intercalated. Dip of stratification is 20°~50° at the top but generally moderate to steep (<50°), and in someplaces vertical.

(6) 688.00 m to 887.50 m: Alternation of grey to grey black chert, grey limestone and black carbonaceous shale is the most dominant rock facies in this section. Thickness of chert bed exceeds sometimes 30 m. Limestone is pale grey to dark grey in colour. The thickness of limestone bed at the upper section is more than 40 m and 10 m at the lower section, where intercalating of dolomitic limestone is present. Black shale occurs generally in the limestone and chert, and in some places 30 m thick banding was found. At some locations the shale becomes pale green and tuffaceous.

(7) 887.50 m to 1,003.00 m: Mainly composed of alternation of chert limestone and tuffaceous mudstone siltstone. Chert is dark grey to black grey colored with intercalated thin layers of black shale. Limestone is dark grey colored and thickness of banding ranges form several meters to about fifteen meters, and black shale layers are often intercalated. Tuffaceous mudstone siltstone has characteristic pale green color with intercalating black shale of several milimeters to several centimeters thickness forming a striped pattern. In the lower part, deeper than 975.00 m, coarse grained sandy shale becomes a member of alternation. Dip of stratification is more than 40°C, averaging 55°C, more or less.

(8) 1,003.00 m to 1,227.40 m: Mainly composed of sandstone with intercalating black shale. Sandstone is grey white colored, medium grain siliceous and quite compact. Silicification by quartz veinlet is common. Black shale is carbonaceous and banded from around 60 centimeters to around ten (10) meters thick and is intercalated in the sandstone. Silicification is common, forming compact hard rock. Dip of stratification is 20° to 50°.

The above-mentioned geology of GTE-7 can be regionally correlated to the lower members of the Kiu Lom Formation of lower permian.

The limestone bearing sequence lower than 158.20 m is lithologically correlated to the similar facies observed in GTE-2, and the sandstone deeper than 1,003.00 m can be correlated to the lower most sandstone of Kiu Lom Formation observed at the west of Wat Pong Hom on the surface.

3.3.3 Alteration

Alteration of GTE-7 is generally weak. Calcite vein and quartz vein both of width less than 10 cm are observed along fissures and joints with accompaning carbonatization and silicification.

Also, a minor amount of pyrite dissemination is common.

From the surface to the depth of 60 m, aside from the argillization caused by the weathering, a limited amount of white clay minerals have been observed suggesting hydrothermal activity occurring in the shallow ground close to the surface. Silicification is marked in the sandstone at the depth of 1,100 m and deeper. There are many portiions with abundant quartz stringers and/or veinlets.

3.3.4 Fractures

To determine the intensity of fracturing, the number of fractures are counted for every 1 m. The distribution of highly fractured zone tends to be limited in such places as contact of two rock types or alternation zone, a part of chert beds and the zone of quartz.calcite veining. Shallow hdyrothermal solution is active between the surface and 60 m depth. The fraotures in this section can be considered as the product of weathering and coincide with presence of shallow groundwater. Among the fractures observed deeper than 90 m, lost circulation occured at two places, i.e., around 455 m and around 1,005 m. Amount of lost circulation was 30 *l*/min at both points.

3.4 Petrological Survey

Various physical characteristics were identified from the rock samples taken mainly from GTE-7. The test items and number of samples are as follows: (Table 3.4-1)

Table 3.4-1 Measurement Result of Rock Materials of GTE-7

No.	Items	No.	Remarks
1.	Thin section study	14.	
2.	X-ray diffraction	14.	
3.	Fluid inclusion	14.	Samples from GTE-2 and 5 are included
4.	Density (3 states)	14.	
5.	Mag Susceptibility	14.	
6.	Heat conductivity	14.	

3.4.1 Observation of Thin Section

The 14 samples studied included 7 samples of sandstone, 6 samples of shale, and one of limestone (Table 3.4-2). The main components of sandstone are allogenic quartz·feldspar and alkali feldspar with accessory allogenic heavy minerals of sphane, zircon etc. Allogenic minerals are subrounded. Sorting of sand grain is good to medium. In the matrix, authigenic sericite are chlorite and observed. Mudstone contains allogenic quartz and plagioclase and authigenic sericite and chlorite. Limestone is muddy and allogenic quartz, plagioclase and authigenic sericite are observed.

Carbonatization is identified in the samples from the depth of 70.05 m, 610.50 m, 663.00 m, 832.00 m, 1,031.70 m, 1,213.50 m. The intensity of alteratioin is medium to weak and the samples from the test well are generally fresh. No silicification is observed in the 14 samples.

3.4.2 X-Ray Diffraction Analysis

All of the samples submited to the X-ray diffraction analysis we studied by microsocpe, except the one sample from the depth of 339.00 m. The results of microscopic stucy reflected those of the X-ray diffraction results (Table 3.4-3). The results of X-ray diffraction will be discussed together with the reuslts of microsocpic study The sample from the depth of 339.00 m seems to have undergone rather strong carbontation and the original rock might be the same lithology as the sample from the depth of 348.00 m studied under the microscope.

3.4.3 Fluid Inclusion Study

The study was done using the samples from GTE-7 and GTE-2,5.

(1) GTE-7

Based on the occurrence of fluid inclusion and homogenized temperature, this test well can be divided into three zones with boundaries established by the points of lost circulation (445 m and 1,005 m).

The fluid inclusion of the upper zone, shallower than 445 m, has high filling temperature; that is, in all of the samples the maximum temperature exceeds 175°C. In the five (5) samples among the eight (8), the maximum temperature exceeds 295°C. Furthermore, the minimum filling temperature of all samples taken from shallower than 200 m exoeed 245°C and the maximum filling temperature of four samples out of five exceeds 295°C. No veining was observed between 455 to 1,005 m. The lower section deeper than 1,005 m includes very fine to fine grained quartz veins with little fluid inclusion. The homogenized temperature is as low as 103°C~116°C.

These three zones of layering determined by the fluid inclusion are comformable with the underground structure obtained by electric well logging.

The electrical logging reveals a disti ct tendency of resistivity; that is, resistivity increases with depth. The resistivity obtained for the lower zone deeper than 1,000 m is as high s the order of 10^3 Ωm and values are relatively less scattered. This is comfomable with the fact that non fracture was observed by core logging. Also it is noteworthy that in the section between 0 m to 400 m, the upper half (shallower than 200 m) shows relatively low resistivity.

In GTE-7, underground temperature was measured upto 1,000 m. Comparing with the three other test wells (GTE-1,4,5) drilled in this area, the characteristics of GTE-7 can be summerized as follows: in the section shallower than 200 m, the test well of the highest temperture is GTE-7. In the seotion between 200 m to 400 m, the temperature of GTE-7 is between that of GTE-1, GTE-4 and GTE-5. In the section deeper than 400 m, GTE-7 is the lowest temperature.

This measured tempeature is comformable with the temperature distribution obtained by the fluid inclusion; that is, the zone above 200 m is undergoing temperature decrease from the stage of the formation of fluid inclusion. As the hot springs are still active, the area belongs to the

discharge zone. Also, the zone between 400 m to 1,000 m belongs to the recharge zone where cold groundwater forms a down flow. For all sections above 1,000 m, fracturing was in evidence from core logging, and electrical logging indicates highly scattered resistivity. Judging from fluid inclusion, data core logging and electrical logging, the zone deepe than 1,000 m may belong to a high resistivity zone with intensive veining of fissure filling quartz.

(2) GTE-2

This well is similar to GTE-7 in showin a decreasing homogenized temperature with depth. The temperature anticipated at 500 m deep may be equal with that at GTE-5. This suggests that the solution altering the zone around GTE-2 may have flowed upward not from direclty below rather from an angle to the side.

(3) GTE-5

The homogenizeded temperature is even from the deep to the shallow level in this test well.

3.4.4 Density Measurement (Table 3.4-4)

Densities of wet rock samples are between 2.60 and 2.75 g/m^3. Some siliceous sandstone has small density of 2.47 g/cm^3. Density is inversely proportional to porosity. The correlation coefficient between density and porosity is rather small, between 0.55 and 4.11.

3.4.5 Magnetic Suceptibility Measurement (Tabl 3.4-4)

Magnetic susceptibility of rocks in GTE-7 is between $6\sim19\times10^{-6}$ emu/cc. It does not vary by rock type.

3.4.6 Heat Conductivity Measurement (Table 3.4-4)

Heat conductivity of rocks in GTE-7 is between $6\sim17\times10^{-3}$cal/cm sec°C. It does not vary by rock type.

3.4.7 Calculation of Heat Flow

Heat flow around GTE-7 is calculated by the following equation.

$$Q = K \times dt/dz$$

where, K (thermal conductivity): 10×10^{-3} cal/cm sec°C
dt/dz = (temperature gradient): 0.4×10^{-3}°C/cm

The calculated heat flow is 4HFU ($\times10^{-6}$ cal/cm^2 sec) and is higher than its the average value for the crust but lower than most known geothermal areas.

3.5 Well Logging

3.5.1 Generalization

During and after completion of drilling, the well, GTE-7, was logged for electric properties and temperature properties.

Well logging was carried out by the well logging vehicle donated to Thailand. The purpose of well logging is to colleot necessary informations to understand physical properties around the well. Well logging is carried out in three stages as shown in the following Table 3.5-1.

Table 3.5-1 Summary of Well Logging of GTE-7

Stage		Items	Remarks
First	200 ~ 500 m	Electric, Temperature	By Thai team
Second	500 ~ 1,003 m	Electric, Temperature (twice), Pressure	Technical advice
Third	1,000 ~ 1,227 m	Electric, Temperature (twice),Caliper, Sonic	Technical advice

The first well logging was carried out in October 1984, after the well was drilled to 504 m and before casing pipe was inserted. The second well logging was carried out in January 1985, after the well was drilled to 1,003 m and before casing pipe was inserted. The third well logging was carried out in March 1985 after the well reached the final depth of 1,227 m.

(1) Instruments

The logging instruments used are as follows:

1) Logging vehicle: Isuzu Foward
2) Cable: outside diameter 9 mm; lengh 2,500 m, 5 conduotors, heat-resistant
3) Temperature logging
   thermometer: absolute temperature 0 to 300°C temperature difference
   probe: outside diameter 45 mm, length 1,600 m (platinum resistor)
4) Electrical logging
   probe: two elements (resistivity and SP)
   outside diameter 45 mm, length 1,750 mm
   (short normal 25 cm, long normal 100 cm)
5) Pressure logging
   pressure gauge: 0 to 200 kg/cm^{2}G
   probe: outside diameter 45 mm
   length 400 mm (strain gauge)
6) Caliper
   meter: 50 to 300 mm (hole diamter measured)

probe: outside diameter 500 mm, length 1,100 mm (tree-arm type)

7) Soni logging

meter: three components (ΔT, amplitude and intensity)

probe: outside diameter 70 mm, length 3,300 mm

(2) Method of measurement

Well logging was carried out by the logging vehicle and the above-mentioned instruments utilizing drilling rigs. Measurement was executed as shown in the following figure (Fig. 3.5-1).

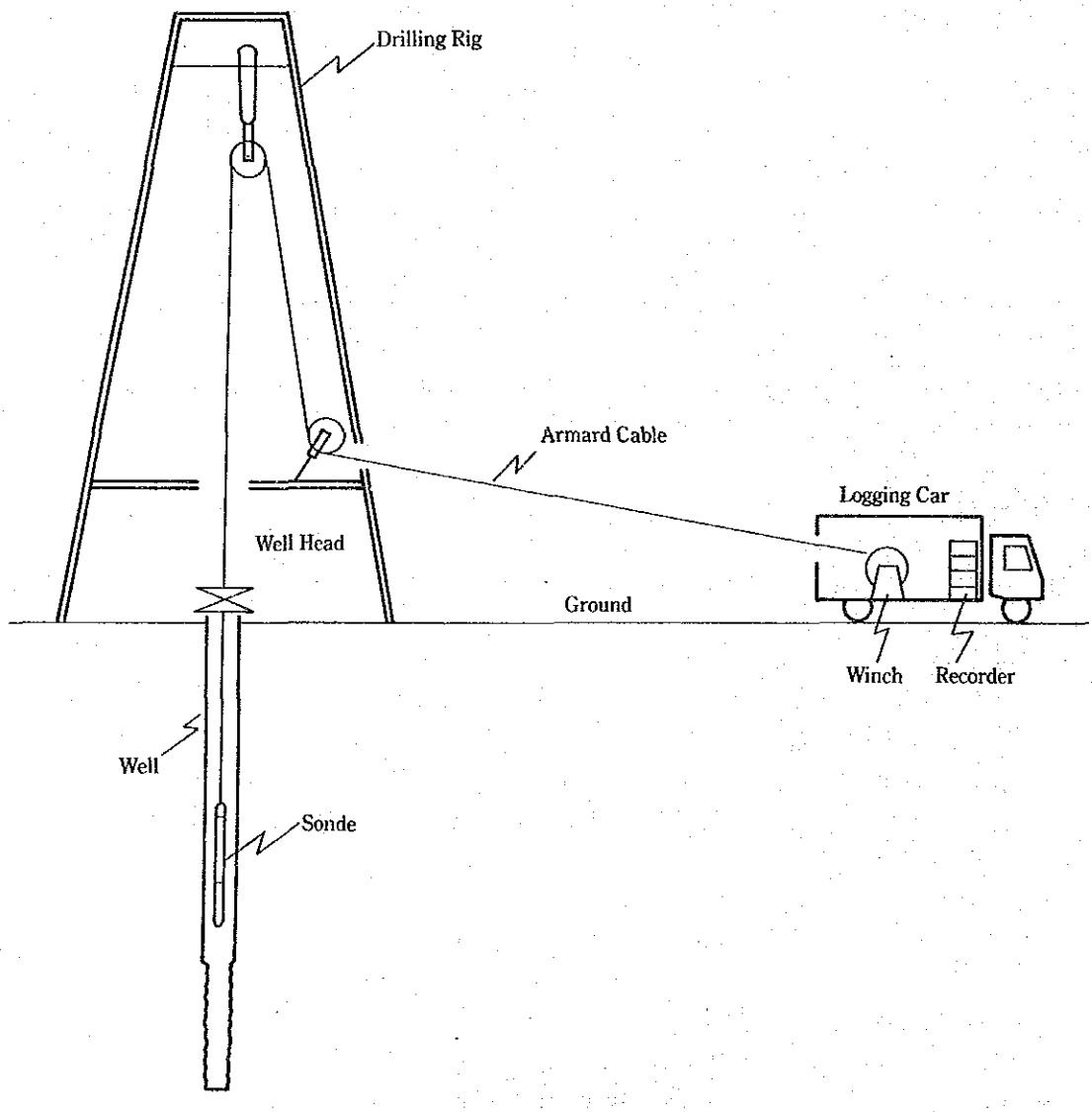

Fig. 3.5-1 Outline of Logging System

Well logging was carried out as follows:

1) Temperature logging

Temperature logging serves to measure temperature change in a hole in the ground continuously (absolute value and temperature difference) be lowering a probe into the hole. It is the most important log for a geothermal well. It serves to study temperature distribution in the hole and that of the geothermal reservoir and to infer heat flow to the surface of the earth from deep ground by using temperature gradient and heat conductance of formations.

2) Electrical logging

Electrical logging to measure resistivity and spontaneous potential of the earth was performed by lowering electrodes arrayed at fixed distances into a drilled hole. Resistivity was measured by the normal electrode array in which electrode separation for long normal was 1,000 mm, and that for short normal was 250 mm. Apparent resistivity measured by long normal represents resistivity of rocks at larger distance away from the hole, and that measured by short normal represents resistivity of rock near the hole. The spontaneous potential method measures electrochemically induced electromotive force at the interface between lutaceous rock and the permeable layer which contacts with the drilling mud in the hole. Electrical logging serves to compare, to identify rock facies and to inter permeability of formations.

3) Pressure logging

Pressure logging serves to measure pressure change in a hole continuously by lowering a pressure probe into the hole. It is used to study pressure of a geothermal reservoir and to infer existence of gothermal fluid in a geothermal reservoir by temperature logging.

4) Caliper logging

Caliper logging serves to measure the hole diameter. Diameter of a hole is not constant and depends on the drilling bit, drilling mud and formations. By measuring hole diameter, location of fractures and change of rock type can be inferred.

5) Sonic logging

Sonic logging serves to study location of fractures and porosites of rocks from record of propagation time, and amplitude and wave shape of ultra-sonic wave transmitted in hole.

3.5.2 Results of Well Logging

Well logging was carried out in three stages. Here, the results of well logging beyond 500 m depth of the second and the third stages, are explained.

(1) Results of well logging in the second stage (Table 3.5-2)

The second stage was up to 1,002.75 m depth and before casing pipe was inserted. (Fig. 3.5-2)

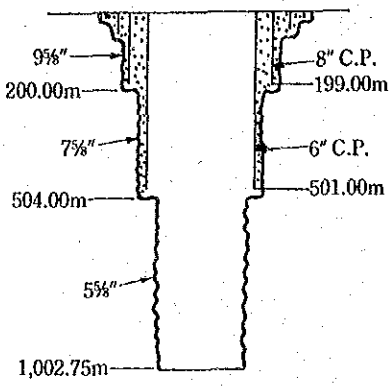

Fig. 3.5-2 Well State in Logging of GTE-7 (Stage 2)

Table 3.5-2 Progress of Well Logging of GTE-7 (Stage 2)

Logging / Items	Electrical logging	Temperature logging		Pressure logging
		First Run	Second Run	
Date	Jan. 9, '85	Jan. 8, '85	Jan. 10, '85	Jan. 10, '85
Drilling depth	1,002.75 m	1,002.75 m	1,002.75 m	1,002.75 m
Casing bottom	6" 501.00 m	6" 501.00 m	6" 501.00 m	6" 501.00 m
Shut in	Jan. 7, '85 8:00	Jan. 7, '85 8:00	Jan. 7, '85 8:00	Jan. 7, '85 8:00
Standing time	—	27 hr	27 hr	—
Time of measurement	15:45 – 16:30	9:20 – 11:00	9:30 – 11:15	14:15 – 15:20
Depth of measurement	500–1,002.75 m	0 – 1,002.75 m	0 – 1,002.75 m	0 – 1,002.75 m
Speed of measurement	10 m/min	10 m/min	10 m/min	10 m/min
Others	—	Max. temperature 90.5°C at the bottom	Max. temperature 90.5°C at the bottom	Max. pressure 105 kg/cm²G at the bottom

The result of well logging are as follow:

① The condition of the well was good. All probes could be lowered to the bottom of the well and all data was recorded.

② Temperature logging shows gentle increase of temperature with depth and no significant change of increase rate. Two measurements of temperature logging, 27 hours and 75 hours

after stopping circulation of cooling water, show no significant temperature change and the temperatures at the bottom of the well for the two measurements are identical. The bottom temperature is 90.5°C.

③ Electrical logging shows resistivity change and SP change corresponding to change of formations. The resistivity log shows high resistivity between 540 m and 570 m, between 700 m and 770 m, between 805 m and 830 m, and between 910 m and 950 m.

④ Pressure logging shows constant pressure increase and the bottom pressure is 105 kg/cm^2G.

(2) Results of well logging in the third stage (Table 3.5-3)

The third stage is down to 1,227.34 m. (Fig. 3.5-3)

Table 3.5-3 Progress of Well Logging of GTE-7 (Stage 3)

Logging / Items	Temperature logging		Electrical logging	Caliper logging	Sonic logging
	First Run	Second Run			
Date	Mar. 1, '85	Mar. 3, '85	Mar. 1, '85	Mar. 2, '85	Mar. 2, '85
Drilling depth	1,227.35 m	1,227.34 m	1,227.34 m	1,227.34 m	1,227.34 m
Casing bottom	1,000.00 m	1,000.00 m	1,000.00 m	1,000.00 m	1,000.00 m
Shut in	Feb. 28, '85 11:00	Feb. 28, '85 11:00	Feb. 28, '85 11:00	Feb. 28, '85 11:00	Feb. 28, '85 11:00
Standing time	24 hr	72 hr	—	—	—
Time of measurement	11:10 ~ 11:40	10:30 ~ 12:00	15:45 ~ 16:30	10:50 ~ 11:15	15:00 ~ 15:20
Depth of measurement	950 ~ 1,227 m	0 ~ 1,227 m	1,000~1,227m	960 ~ 1,227 m	950 ~ 1,228 m
Speed of measurement	10 m/min	10 m/min	10 m/min	10 m/min	10 m/min
Others	Max. temperature 99.4°C at the bottom	Max. temperature 99.8°C at the bottom	—	—	—

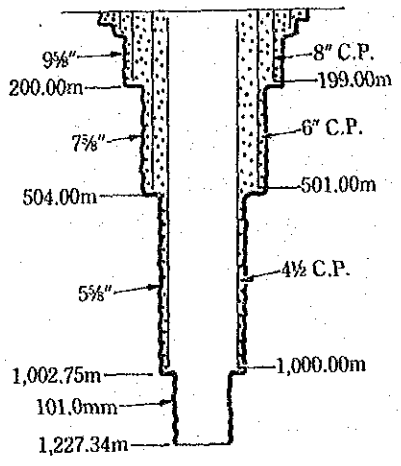

Fig. 3.5-3 Well State in Logging of GTE-7 (Stage 3)

The result of well logging are as follows:

① The condition of the well was good. All probes could be lowered to the bottom of the well (1,227m) and all data was recorded.

② Temperature logging shows no sudden change of temperature as with the second stage. The maximum temperature at the bottom is 99.8°C and is a temperature after recovered.

③ Electrical logging shows relatively high resistivity which implies existence of very hard rocks. Especially at near the bottom, resistivity is very high over 2,500 Ωm.

④ Caliper logging shows no change of the well diameter which implies wall of the hole being well retained.

⑤ Sonic logging shows existence of very hard formations for which sonic speed is as fast as that for iron pipe. The intensity logging shows no existence of cracks. The amplitude also shows no significant change.

(3) Summary

The result of well logging in GTE-7 are summarized as follows:

1) Temperature logging

Temperature logging was run several times during drilling. The final temperature logging run, recorded after drilling reaching to the bottom of the well (1,227 m), is shown in Fig. 3.5-4. The final temperature logging was run 72 hours after the water pump stopped and temperature condition of the well was thought to reach equilibrium with that of surrounding formations.

Temperature between 20 m and 30 m deep is relatively high at 65°C, but between 30 m and 150 m decreases with depth. Beyond 150 m, temperature increases with depth, but temperature gradient is very gentle. The bottom temperature is relatively low, about 100°C.

2) Electrical logging

Resistivity and spontaneous potential against depth are shown in Fig. 3-5-5.

To the depth of 1,001 m where casing pipe was inserted, the resistivity logs of both

long and short normal show variety and high values in the zones between 540 m and 570 m, between 700 m and 770 m, between 805 m and 830 m, between 865 ma dn 890 m, and between 910 m and 950 m. In other parts, resistivity is low (under 100m).

In the depth beyond 1,000 m, resistivity varies in the zones between 1,010 m and 1,030 m, between 1,140 m and 1,160 m, between 1,175 m and 1,215 m and between 1,220 m and 1,227 m. Especially in the zones between 1,010 m and 1,030 m, between 1,175 m and 1,215 m and between 1,220 m and 1,277 m, resistivity is high.

In the well, high resistivity zones and low resistivity zones appear alternatively. Resistivity around 1,200 m deep is over 2,500 Ω-m.

Because of high resistivity, sonic logging results, and drilling conditions, geologic formations in the well are assumed to be very hard.

3.6 Re-Interpretation of Result of Deep Electrical Survey

3.6.1 Correlation of Result of Deep Electrical Survey With Electrical Logging

The trajectory of the GTE-7 well, as indicated by a single shot measurement of orientation and inclination, shows that the deviation of well bottom from well head is between 173 and 160 m. Comparison of this trajectory with resistivity cross sections obtained from the MT method survey results revealed that GTE-7 does not penetrate a low resistivity zone which had been indicated by the MT survey and instead, its well bottom locates in a formation whose resitivity was estimated to be about 26 ~ 36Ω-m.

Comparison of actual trajectory of the well with the results of the MT survey is shown in Fig. 3.6-1.

Then, the results of electrical logging in GTE-7 were compared with the MT survey results. Since resistivity values from the electrical logging were not absolute values but ones by the influence of drilling mud impedance, the comparison of the tendencies f both results was given emphasis. Fig. 3.6-11 shows the comparison between the electrical logging results and MT survey results, and the following outlines a conclusion from the comparison.

(1) In the well, formations are alternated and electrical logging results show a very wide scatter in resistivity, which ranges from around 5 Ωm-m to around 5 thousand Ωm-m. MT survey reults reflected the lower resistivity formations of those so alternated This derived from the nature of the principle of the MT method. The method is far more sensitive to lower resistivity levels, and alternated formations of high and low resistivity are reflected in the MT survey results not as an average level but as a resistivity value more deviated to the lower side.

(2) The tendency of resistivity distributionof the electrical logging results and that of MT survey results correspond with each other, although the former is slightly high as compared with the latter.

(3) A trend of considerable rise in resistivity, which the electrical logging results showed near the bottom of the well, is understood to reflect a part of the alternated formations that also

include low resistivity parts.

(4) In spite of a very wide scatter in resistivity observed in the electrical logging results, they generally s ow higher resistivity as depth increases. A similar trend is exhibited by the MT survey results although some discrepancies with the former results are found in tems of depth.

(5) It is true that the current MT method interpretation cannot always provide a sufficiently fine resolution level to identify vertically varying physical properties of rocks that form thin layers. In spite of this, the re-analysis and re-displaying of MT method results taking account of such complex geology, is possible and is deemed to be effective for providing more useful information.

3.6.2 Method of Analysis

(1) Objectives and outline of Re-interpretation process

The MT interpretation process outlined in the proceeding section was on the total conductance values of individual stations, and also on the distribution maps of total conductance.

The result of electrical logging in GTE-7, and the results of the MT method interpretation in the preceding survey showed generally similar trends. However, it was pointed out that the high complexlty of geological structure in this survey area would require review and re-interpretation of the MT survey results to more effectively exploit survey data.

To meet this requirement, automatic iterative analysis was employed this time for the one-dimensional model interepretation, and the resultant theoretical curves were used for Bostick inversion. In this new attempt, the Bostick inversion results were employed to obtain contoured resistivity maps and cross sections, which showed gradual change of resistivity in vertical and horizontal directions, and indicated discontinuities and contrasts in resistivity, in the survey area.

At the same time, electrical basement maps were outputed from the one-dimensional models to identify discrepancies and discontinuities of the basements.

The sequential procedure of this re-inter is shown by flow chart in Fig. 3-6-2.

(2) Analysis of the one-dimensional model

Automatic iterative analysis was used for this one-dimensional model resistivity interepretation. This analysis employed the least method procedure and sought formation parameters that corresponded to the measured MT survey curves, by improvement through repetition. Formation parameters at individual measuring points were described by thickness and resistiviy of each formation.

Figure 3.6-3 illustrates a typical exampl of resistivity interpreation through one-dimensional modeling, and that of theoretical apparent resistivity curve (matching curve) obtained from a one-dimensional model.

(3) Bostick inversion

It was concluded that, in the case of finely varying rock properties in the ground as observed in the formations of this survey, a contoured resistivity distribution map through the Bostick inversion would be more useful for interpretation than an output from the one-dimensional model resistivity interpretation. At the same time, the problem that a Bostick inversion tends to show the influence of data scatter was strongly pointed out (Fig.3.6-4).

For these reasons, Bostick inversion was applied this time to a matching curve which resulted from the one-dimensional model resistivity interpretation, with a view to abating the influence of scattered data on the interpretation, and ensuring consistency between the Bostick inversion results and the one-dimensional model resistivity interpretation results.

The Bostick inversion includes a technique to transform an apparent resistivity to a true resistivity and depth by the inversion method. This inversion is based on the asymptotic feature of an apparent resistivity curve in the low frequency zone, and obtains true resistivity values through comparison of an asymptotoic curve of the apparent resistivity with the tilt angle of the asymptotoic line when electric basement is made of perfectly conductive or perfectly insulated material (−1 or +1) respectively.

An apparent resistivity can be transformed to a true resistivity and depth by the following two expression.

$$\rho = \rho a \frac{1 - \frac{d(\log \rho a)}{d(\log \omega)}}{1 + \frac{d(\log \rho a)}{d(\log \omega)}}$$

$$D = \rho a / \omega \mu$$

where,

ρa : apparent resistivity (Ω-m)
ρ : true resistivity (Ω-m)
D : skin depth (m)
ω : angle velocity (rads/sec)
μ : magnetic susceptibility ($4\pi \times 10^{-7}$ H/m)

(4) Resistivity map and resistivity cross section

A contoured resisistivity map indicates contoured iso-resistivity lines for a specific depth, as obtained from Bostick inversion results at individual measuring points, and the horizontal distribution of resistivity at a given depth in the survey area.

A contoured resistivity cross section has contoured iso-resistivity lines as determined at a pre-set depth interval across a vertical profile under a specific survey line, and reflects the vertical distribution of resistivity under the given survey line.

(5) Preparation of electrical basement map

The interpretation results of a one-dimensional model are useful for classifying geological formations. They serve better and are more convenient for illustrating the vertical distribution and shapes of ectrical basement corresponding to basement rock.

In this survey, the depth of the top of every high resistivity zone, having above 1,000 Ω-m as a rule, was acquired from the interpretation results of the one-dimensional model for individual measuring points, and an electrical basement maps was drawn with the iso-depth lines of such zone top levels.

3.6.3 Results of Analysis

The results mainly of the re-interpretation perfomed after drilling of GET-7 are outlined below because the complex geological structure, often observed in areas like this survey area, can be better described by the results from the re-interpretation which mainly contain the stepped vertical and horizontal variations of resistivity, and the discontinuity contrast in resistivity.

(1) Resistivity maps (Fig. 3.6-5 to Fig. 3.6-8)

One resistivity map was obtained for each of four depths (+200 m, −500 m, −1,000 m, and −3,000 m above sea level)

The following is the outline of the local conditions in relation to all these maps.

1) Some low-to-moderate resistivity zones can be observed at every depth level, with Wat Pong Hom as ts center. These zones are surrounded be high resistivity zones, with a border line approximately passing sations 2-1, 104, 3-3, 2-3, 1-3, and 105. The distribution range of these low-to-moderate resitivity zones are observed to be shifted slightly toward the northwest in the resistivity map of SL-3,000 m. In these low-to-moderate resistivity zones, resistivity level is seen tending to increase with depth.
2) To the southeast of Ban Mae Khu Ha, and particularly at and around station 3-4, a high resistivity zone is identified to every depth, but its range tends to become smaller at greater depths (SL-3,000 m). In the vicinity of the center of this high zone, resistivity level exceeds 1,000 Ωm, and the zone exhibits a conspicuous contrast to the low resistivity zone around Wat Pong Hom and also to the low zone around Wat Hua Fai and Wat Nong Hoi described below.
3) In the eastern part of the survey area, a considerably wide area of low-to-moderate resistivity zone is observed around Wat Hua Fai and Wat Nong Hoi, and the area shows a clear contrast to the high resisitvity zone method above. In the shallow level, this low resistivity zone mainly lies in the southeast part of the survey area, and tends to extend northward with lower resistivity level as depth increase.
4) In the vicinity of Ban Nong Bo Yen, Ban Mae Hong Khrai and Doi Luang in the northwest part of the survey area, a high resistivity zone is identified at every depth.

(2) Resistivity cross sections (Contoured) (Fig. 3-6-10~12)

A resistivity cross section was obtained for each of the three survey lines (Lines 1, 2 and 3). A

location map of the survey lines is shown in Fig. 3.6-9. Resistivity distribution on the individual cross sections are outlines as follows:

1) Survey line 1

This survey line was set so that it may pass Huai Pong, Wat Pong Hom, and Ban Pong Hom along a single line from south to northeast (passing stations 0-2, 1-2, 105, 2-2, 106, 3-2, 107, and 4-2).

A low resistivity zone lies around station 2-2, and resistivity levels in the zone tend to rise as depth increases.

In the vicinity of station 105, a substational discontinuity of resistivity is identified, and around station 106, another such discontinuity is found.

A high resistivity zone is observed in the vicinity of station 0-2, 3-2 and 4-2. The high zone around the station 3-2, in particular, tends to continue down to deep ground.

2) Survey line 2

This survey line was laid so as to pass Ban Mae Hong Khrai, Ban Pong Nok, and Ban Hua Fai along a single line running from northwest to southeast (passing stations 1-0, 1-1, 102, 105, 108, 2-3, 111, 2-4, 3-5, 3-6, and 118). This survey line approximately corresponds to the seismic exploration line A.

A low resistivity zone is seen in an area around stations 105 and 108, although the zones under the two points are different in depth.

A substantional discontinuity of resistivity is identified between station 108 and station 2-3, and another one in the vicinity of station 101. Both tend to reach to deep ground.

3) Survey line 3

With this survey line, the eastern part of station 2-3 was set so as to be identical with Survey Line 2, but its western part proceeded in the north-to-southeast direction to pass was Pong Hom (passing stations 101, 2-1, 03, 2-2, 109, 2-3, 111, 2-4, 3-5, 3-6 and 118).

A low resistivity zone lies around station 2-2, and its resistivity level tends to rise as depth increases.

A substantial discontinuity in resistivity is identified approximately between station 109 and station 2-3, and another one around station 2-4, and in both cases the discontinuities tend to extend down to deep ground.

Yet another substantial discontinuity of resistivity is seen around station 2-1, and across this point, a high resistivity zone around station 101 exhibits a sharp contrast to a low zone around station 103 and 2-2.

(3) Electrical basement map (Fig. 3.6-13)

The depth to the top border of individual high resistivity zones having a resisistivity level of, in principle, 1,000 Ω-m or higher, was obtained from resistivity cross section maps (shown in blocks) based on one-dimensional model resistivity interpretation. All the zone top depth levels were contoured by iso-depth lines and an electrical basement map prepared. The distribution of electrical basement can be outline in relation to th map, as follows.

- In the low-to-moderate resistivity zone, having Wat Pong Hom as its center, the electrical

basement is shallower than in the surroundings of the zone, indicating the presence of a rise in the electrical basement. Substantial bends in electrical basement contours are identified around staitons 102, 103, 106 and 108.

- The shallow electrical basement, referred to above, extends continually eastward to the high resistivity zone around Ban Mae Khu Ha, and substantial discontinuities in electrical basement are found in the vicintiy of stations 111 and 3-4.

(4) Summary

On the basis of the re-interpretation results, the structure of resistivity in this survey area can be summarized as follows.

1) A low-to-moderate resistivity zone is identified, with Wat Pong Hom at its center. This zone coincides with a rise of electrical basement. A radical drop of electrical basement is found along the north edge of this low-to-moderate zone. According to drilling results of GTE-7, this zone seems to correspond to alterated formations of volcanic rocks and clay which all represent low resistivity. The radical drop of electrical basement along the north edge may be due to some fracture system, as this is indicated by a discontinuity in resistivity, which continually extends from shallow to deep ground in the resistivity cross sections.
2) A high resistivity zone is observed to the southwest of Ban Mae Khu Ha. Resistivity in the center of the zone exceeds 1,000 Ω-m, indicating the presence of considerably tight rocks. This zone coincides with a rise of electrical basement, along the southern rim of which a radical drop of electrical basement occurs, suggesting that a fracture system exists along the rim.
3) In the vicinity of Wat Hua Fai and Wat Nong Hoi in the eastern part of the survey areas, a comparatively wide range of low-to-moderate resisitivity zone is identified, with its area more and more extensive resisitivity tending to lower, as depth increases. It is not clear whether this low-to-moderate zone reflects alternate formations of low resistivity like the area around well GTE-7, or otherwise, the presence of some fracture system.
4) High resistivity zones are identified in the vicinity of Ban Nong Bo Yen, Ban Mae Hong Khrai and Doi Luang in the northwest part of the survey area. All these high zones correspond to a rise in or extension of the electrical basement.

3.7 Consideration on Distribution of Down Hole Temperature

3.7.1 Generalization

The most distinguishing characteristic in the subsurface temperature distribution is the gradual rising of the temperature which is proportional to the depth and the fact that he temperature gradient is only 4°C/100 m (1°C/25 m). This value is a rather small value.

Another characteristic is that the temperature near the surface (depth shallower than 150 m) is higher than that of the deeper layer. This phenomenom is considered to be the effect of hot water in a gravel layer and weathered basement rock near the surface because the location of this exploratory well is near the geothermal manifestations. However, it must be emphasized that the temperature at 150 m depth is observed as high as 60°C and that the cooling effect at shallow depth as observed near the surface at the other survey wells is not in evidence.

In general, for survey well without any blow-out the area may form a shallow high temperature zone caused by the thermal water from the hot spring nearby. However, as depth increases, the temperature becomes lower than that at the surface due to cooling effect.

However, the temperature of the GTE-7 exprloratory well is found to be as high as 60°C even at 150 m depth from the surface and the thermal gradient of the deeper zone is not as large as expected despite the short distance from the geothermal manifestation area. This phenomenon cannot be attributed to simple thermal conduction as in the case of other exploratory wells except for GTE-2 and GTE-6. Consequently, it seems to be necessary to find the reason for this phenomenon (temperature distribution anomaly) by pursuing it from a different angle.

3.7.2 Geothermal System and Terestrial Heat Flow

Where a geothermal water system exist, there may be two zones, i.e., one is the thermal water discharge area with high heat flow zone, and the other is the water recharge area near the thermal water discharge area with a low heat flow zone, the two zones being characterized by differences in heat supply intensity. In the recharge area, the temperature is low and the temperature gradie t is also small. In the discharge area, the temperature is high near the surface because of the rising thermal water, but the temperature gradient is generally small.

3.7.3 Model of the Geothermal System in the San Kampaeng Area

The geothermal system in the San Kapaeng area lies between the NNW-SSE trending Huai Pong and Ban Mae MKhu Ha faults. The present geothermal manifestation area consists of the discharge area and the surrounding recharge area. In the recharge area, the water that penetrates into the fault and/or into the permeable layer may include ground water as well as spring water near the surface of the geothermal manifestation area. In addition to the above-mentioned factors, the following two features are seen in the temperature distribution in the GTE-7 survey well.

(1) The temperature in the survey well is not as high as expected despite its location near to the geothermal manifestation, and also the temperature gradient is small.

(2) On the other hand, the temperature at 150 m depth, where little influence of surface water is assumed, is rather high.

Judging from these factors the temperatur distribution in the GTE-7 exploratory well seems to indicate that of the recharge area outside the discharge area.

3.7.4 Effect of Descending Water on Underground Temperature

(1) Basic equation

Assuming the water penetrates downward from the ground surface through fine pathways, and then subsequently returns to the surface, the change of temperature during penetration to depth (DE) is described by the following equation.

$$q\rho c\frac{d\theta}{dz} = 2\pi r_0 h'' \{\theta-[\theta_0''+\alpha(D-2)]\}$$

where,

θ :	water temperature in pipe
q :	flow rate
ρc :	specific gravity and specific heat of water
r_0 :	radius of pipe
h'' :	cooling constant
Z :	depth of penetration
θ_0'':	temperature of ground surface (= temperature of penetrating water)
α :	gradient of underground temperature change

When Z=D and $\theta=\theta_0''$, the solution of the above equation becomes the following:

$$\theta = \theta_0''+\alpha(D-Z) - \frac{\alpha}{r}\{1 - \exp[-r(D-Z)]\}$$

When Z=0, then the water temperature at the end of the pipe will be calculated by the following equqation:

$$\theta b = \theta_0''+\alpha D - \frac{\alpha}{r}[1 - \exp(-rD)]$$

where, $r = \frac{2\pi r_0 h''}{q\rho c}$

This equation is the basic equation to calculate the water temperature at the penetrating depth D.

(2) Matching temperature with the GTE-7 survey well temperature distribution

It is considered that recharge are water penetrates into the ground through small fissures, instead of a great deal of water genetration occurring through one large channel, and that these small fissures form the so called recharge area.

Therefore, the total amount of the penetrating water is the summation of the descending ground water through the small fissures. In the case of the San Kampaeng area as well since it consists of hard rock, the penetrating water probably descends into the deep ground through small fissures as described above.

Hence, in the reoharge area, the emperature of the geologic formation may become lower than the original temperature because the descending water from the surface may have a cooling effect on the the rock. In other words, it is possible that the temperature distribution in the GTE-7 exploratory well reflects the temperature of the cooled geologic formation.

Based on the above-mentioned consideration, the matching of the calculated temperature distribution with the present temperature distribution in the GTE-7 exploratory well was carried out to find the conditions for the hot water penetration whereby the same temperature distribution

by cooling as the temperature in the present exploratory well is achieved.

For this purpose, various values for the following parameters were applied:

α = primary temperature distribution
r_0 = size of fracture
θ_0'' = temperature of penetrating water
q = quantity of penetrating water

And the basic equation mentioned above was used to calculate water temperature (θb) at depth (D). The calculated temperature distribution is compared with the temperature distribution in the GTE-7 exploratory well to see the degree of approximation. If the approximation is found to be good, then the above-mentioned assumption may be considered as reasonably valid. Among the calculations done to date, one set of results are shown in Fig. 3.7-1 where temperature distribution shows rather good agreement with the actual temperature distribution in the GTE-7 exploratory well.

where,

α : 1°C/9 m (approximately the same temperature gradient as GTE-5 1°C/8.3 m)
r_0 : 2 cm (the radius of a fine pathway)
θ_0'' : 60°C (the temperture of hot spring water at the depth 150 m in GTE-7)
q : 20 *l*/min (the same value as the penetrating rate of water deeper than 1,005 m)
ρc : 1 cal/cm^3·°C
h″ : 0.25×10 cal^{-3}/cm^2·sec°C

In Fig. 3.7-1, the calculation for matching is performed on the assumption that the temperature distribution under the ground shallower than 150 m is equal to the actual temperature disribution in the GTE-7 exploratory well, and hot water of 60°C temperature penetrates deep underground from this depth. In the figure, (A) shows the temperature distribution in the GTE-7 survey well. (B) shows the temperature gradient and (°C) shows the calculated temperature distribution curve at each depth. The calculated results and the measured temperature in GTE-7 at various depths are compared in Table 3.7-1.

Table 3.7-1 Result of Matching between Calculated Temperature and Measured Temperature for GTE-7

Penetration Depth	Penetration Water Temperature	Temperature in GTE-7 Survey well	Difference
150 m: 0 m	60°C	60°C	0°C
400 m: 250 m	63°C	70°C	-7°C
650 m: 500 m	71°C	77°C	-6°C
900 m: 750 m	83.5°C	87°C	-3.5°C
1,150 m: 1,000 m	99°C	97°C	+2°C
1,227 m: 1,077 m	104°C	104°C	+4°C

The temperature difference between the calculated temperature and the measured temperature in the table shows that slighty lower calculated value results than the actual observed value above 1,150 m, and a slighty higher calculated value results than the actual observed value below this depth. However, in general, the calculated value approroximates the measured temperature distribution in the GTE-7 exploratory well. In this calculation, the assumption is made that hot water of 60°C penetrates through fine pathways of 2 cm radius and that the flow rate is 20 *l*/min.

Although the total amount of water penetrating from the recharge area is not known the water is assumed to penetrate from the recharge area through fissures in the high temperature rock mass causing lower underground temperature resulting in the characteristics of the temperature distribution observed in the present GTE-7 exploratory well.

3.7.5 Model of Geothermal System Revised by Drilling of GTE-7

The results obatined by the GTE-7 boring are described as follows.

① Fissures are found in the low resistivity zone of less than 5 Ω-m.
② On the other hand, from the temperature distribution analysis of the survey well the boring site is considered to be the recharge area of hot water.
③ Hence, even if GTE-7 boring encounters a large fracture, it is predicted that the water temperature would not be enough to merit consideration.
④ The location of GTE-7 boring seems to be in a low temperature zone, and the location where the geothermal manifestation exists seems to be a high temperature zone. Therefore, a fault of NE-SW direction is expected between the two zones.
⑤ In other words, the initial GTE-7 boring site seemed to be an existing hot water zone (discharge area), and the low resistivity zone of 5 Ω-meter corresponding to that discharge area.
⑥ However, actual boring results suggest hat the GTE-7 area is a recharge area of hot water, with fluid penetrating into the ground from this area through the estimated fault and accompanying fractures described in Clause 3.7.4.

From the above-mentioned the initially assumed concept of the geothermal system required amendment, as it became clear that the location of the discharge area with high temperature water i.e., the geothermal reservoir, is limited to the area to the south beyond the amended predicted fault in NE-SE direction. The concept of the horizontal geothermal system model is shown in Fig. 3.7-2.

3.8 Summary

Based on the result of GTE-7 core survey, the geological structure was reviewed and it was revealed that the subject geological structure is rather a monoclinic structure, instead of the initially assumed anticlinic structure extending in the vicinity of GTE-2. It is also estimated that a fault exists in NE-SW direction between the geothermal manifestation area and GTE-7.

The results of the resistivity survey in the exploratory well and the result of the specific resistivity cross section by the one dimensional analysis carried out at this stage as well as the previous result of the two dimensional analysis by MT method are compared. The result of the resistivity survey in the exploratory well and the result of the resistivity cross section by the one dimensional analysis suggest an alternation of high specific resistance layers. However, the result of the two dimensional analysis by MT method suggests a low resistivity later. This is because the two dimensional analysis by MT method strongly indicates the effect of low resistivity laters, with poor resolution for high specific resitivity layers even if such are actually present.

Therefore, the results of the GTE-7 boring suggest that the location of the bottom of the survey well is slightly outside of the low resistivity layer estimated from the results of two dimensional analysis by ME method because of the slight bending of the bore hole.

However, the problem regarding the temperature distribution in the GTE-7 exploratory well is that the underground temperature remains about 100°C at its maximum, even at the bottom of the well at 1,227 m depth, despite the location of the boring site near to the geothermal manifestation area. Therefore, it was concluded that, from analysis of the temperature in the survey well, the area near the GTE-7 survey well is a recharge area of hot water of temperature about 60°C since this relatively high temperature was found at 150 m depth.

The scale of the recharge area is not clear yet; however, there is a possibility that the fault in NE-SW direction at the north of the geothermal manifestation area estimated from the boring is the boundary of the recharge area.

In any case, boring at GTE-7 was concluded as indicating that the measurement point 2-2 by the MT method is in a low temperature area. To define the precise scale and location of the geothermal reservoir in the San Kampaeng area, it is necessary to conduct further boring in and around the geothermal manifestation area in order to identify the faulting which serves as the pathway for rising geothermal fluid and to confirm the temperature of the geothermal fluid.

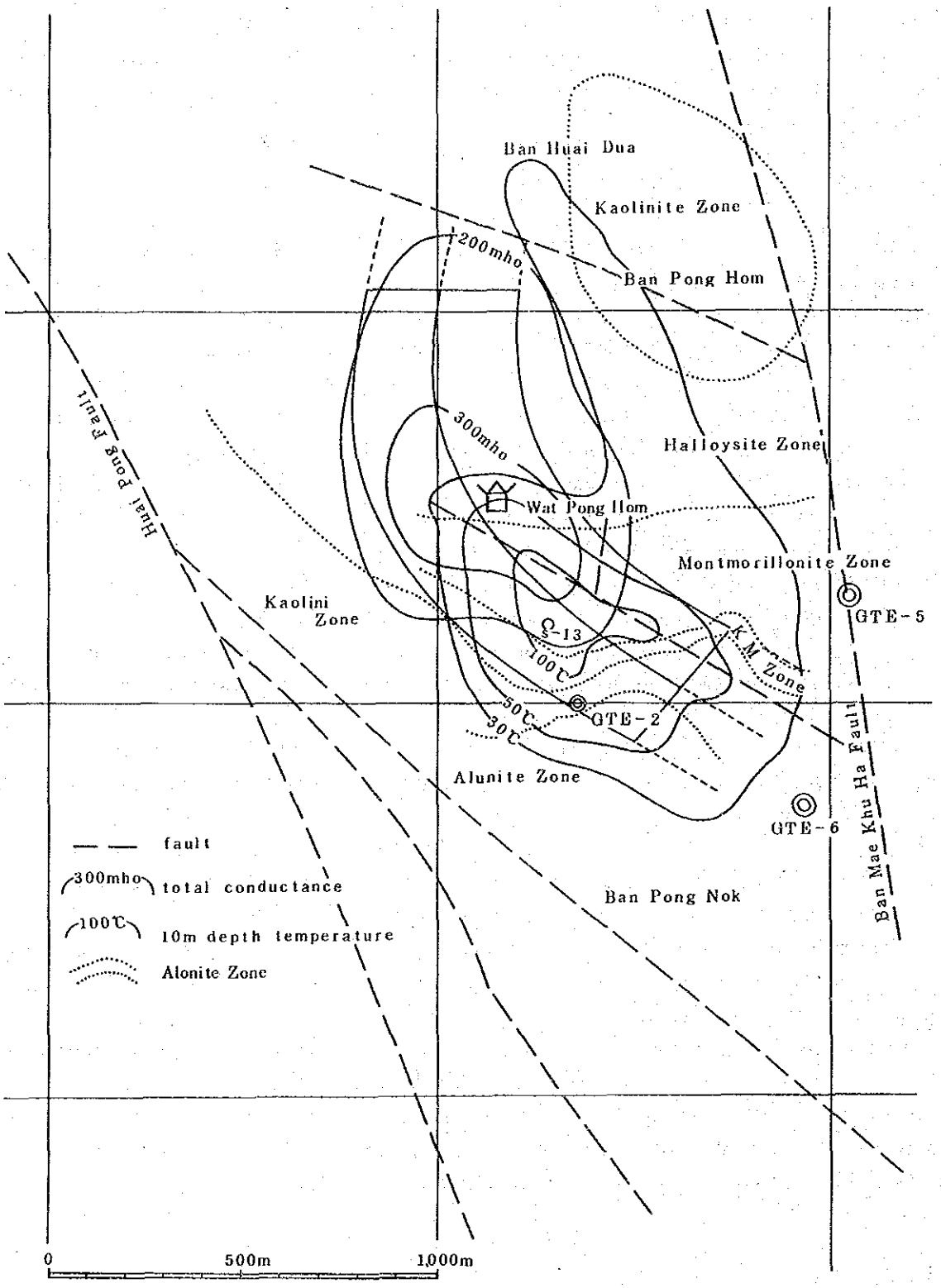

Fig. 3.1-1 Compile Map of Surface Survey (1983)

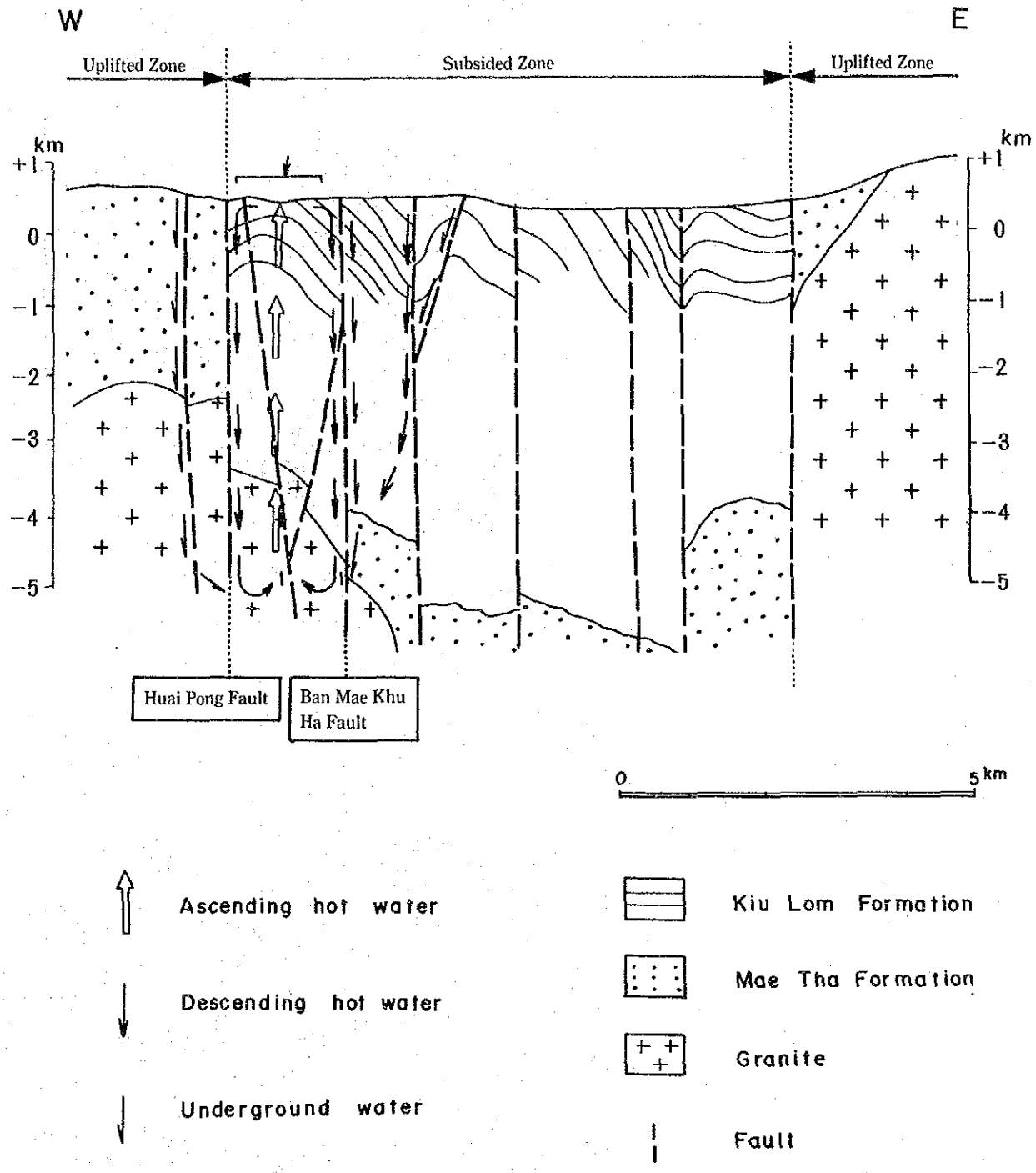

Fig. 3.1-2 Geothermal Model of the San Kampaeng Field

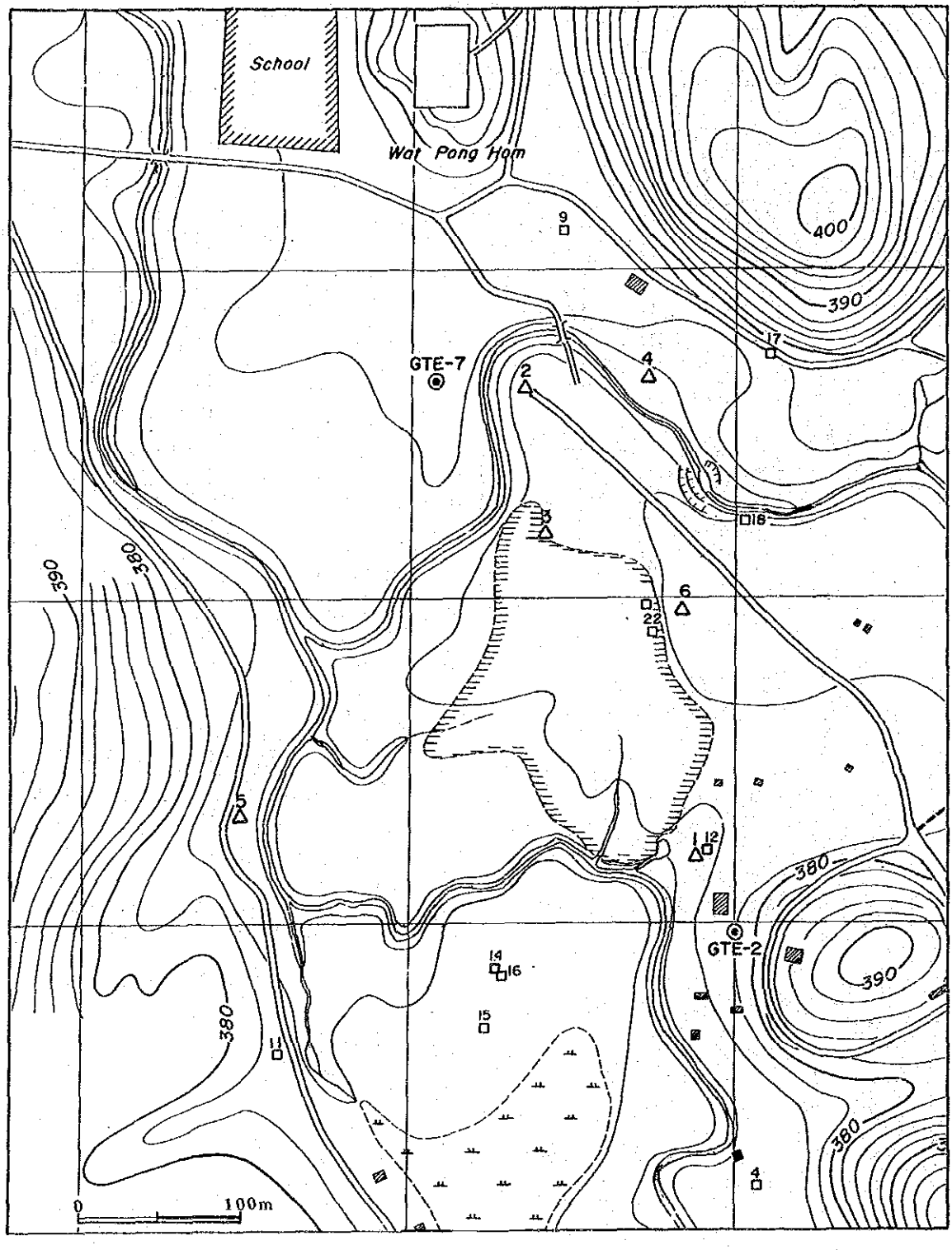

Fig. 3.2-1 Location of GTE-7

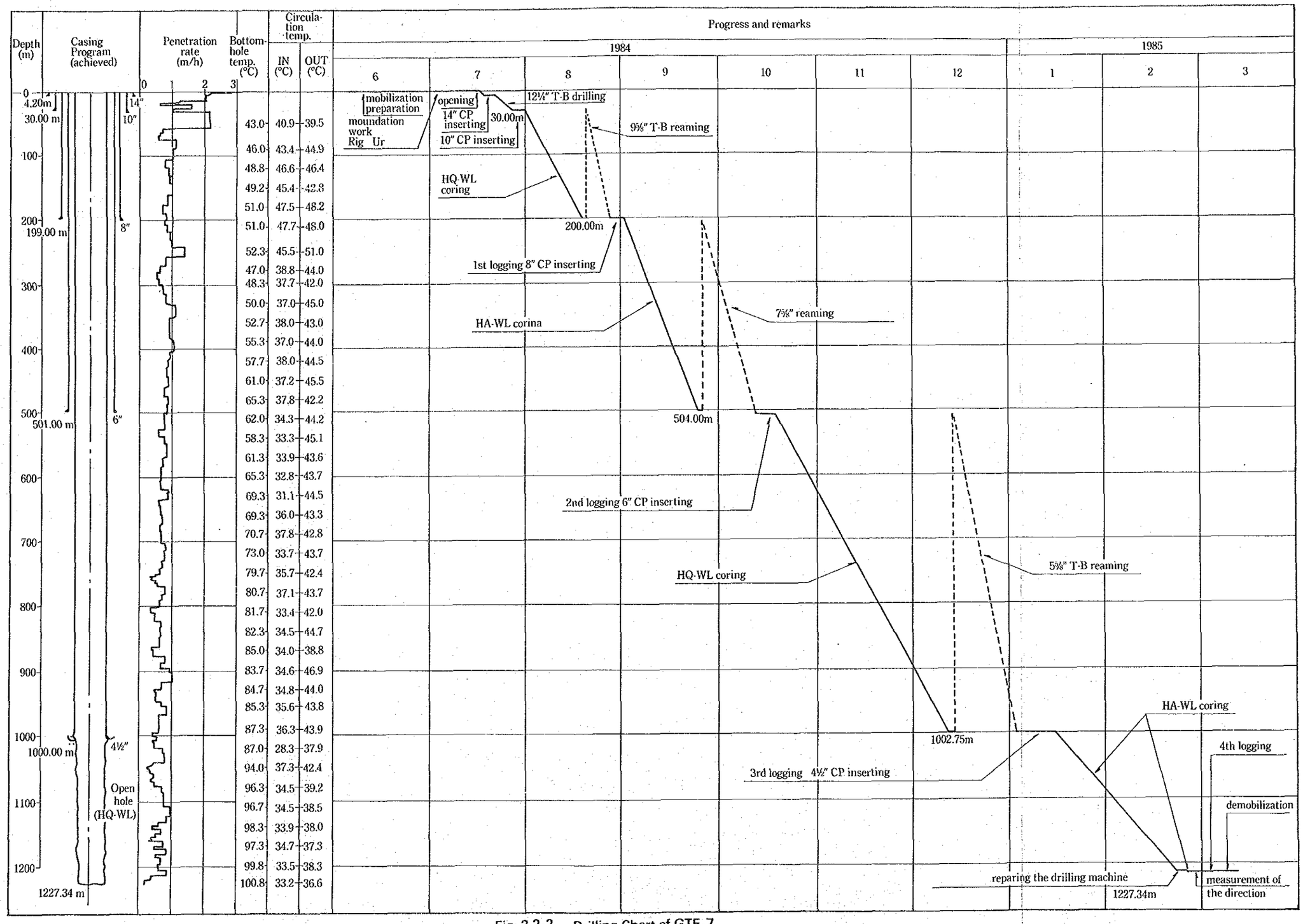

Fig. 3.2-2 Drilling Chart of GTE-7

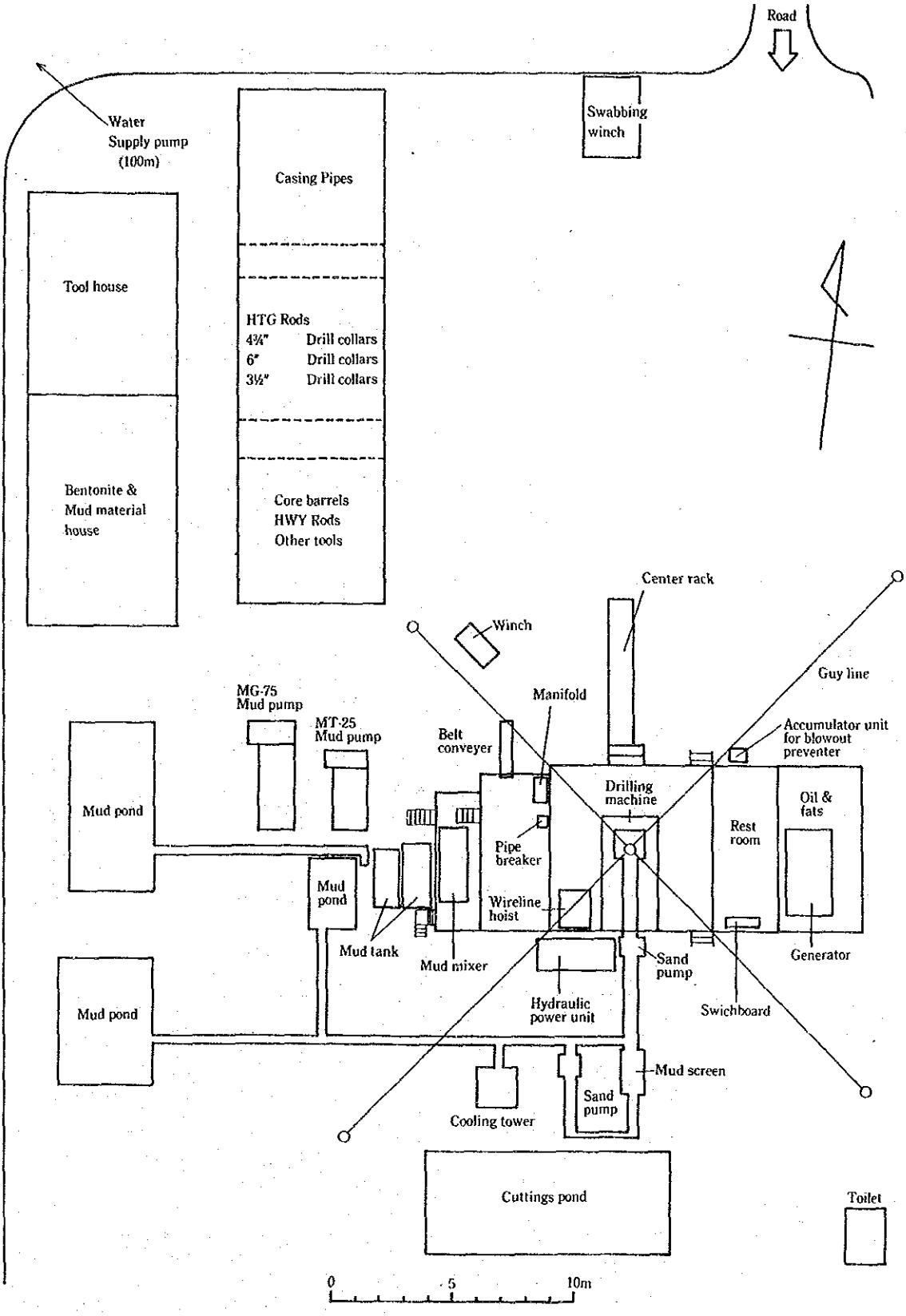

Fig. 3.2-3 Lay out of Drilling Site of GTE-7

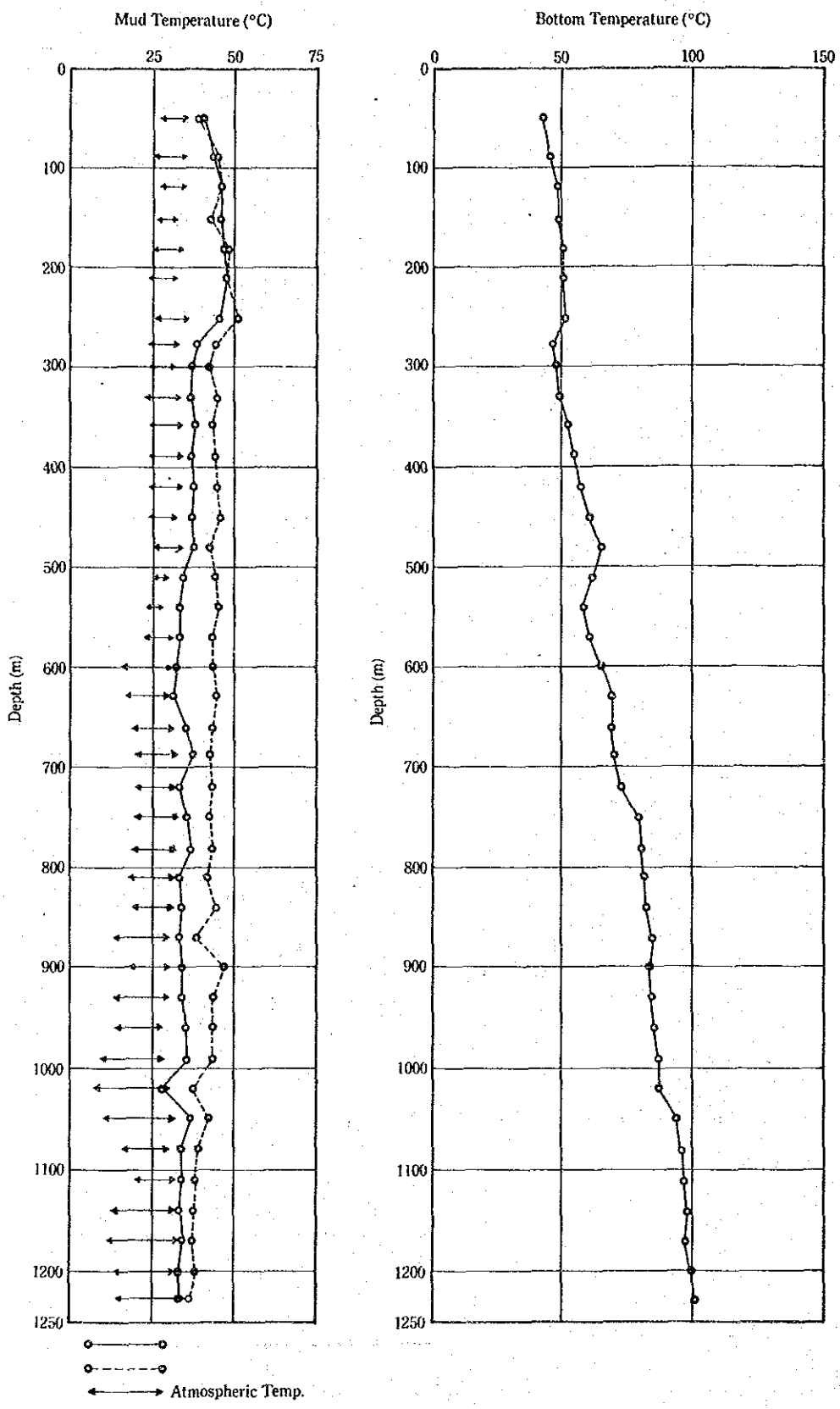

Fig. 3.2-4 Result of Mud Temperature Measurement

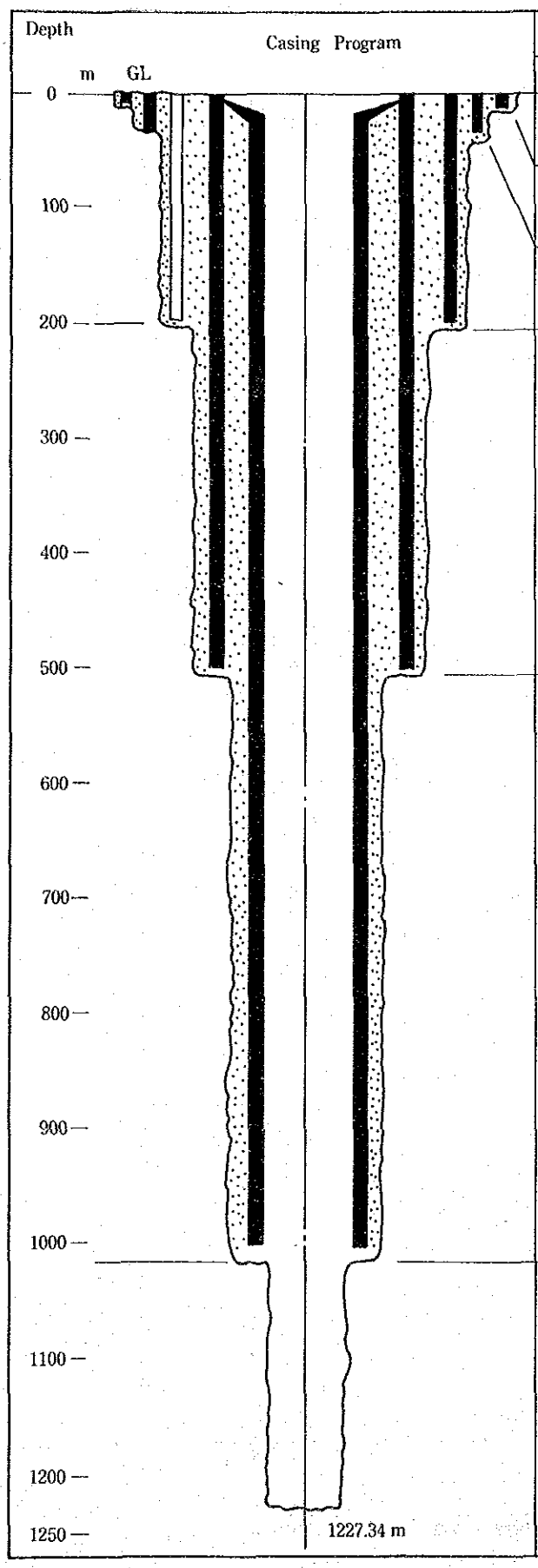

Casing Program

Drilling		Casing inserted	
Hole diam.	Depth	Size	Depth
14″ SCT (357.6mm)	0m ~ 4.20m	14″ SGP	0m ~ 4.20m l = 4.20m
12¼″ (311.2mm)	4.20m ~ 30.00m	10″ SGP	0m ~ 28.10m l = 28.10m
9⅝″ (244.5mm)	30.00m ~ 200.00m	8″ STPG-38 Sch 40	0m ~ 199.00m l = 199.00m
7⅝″ (193.7mm)	200.00m ~ 504.00m	6″ STPG-38 Sch 40	0m ~ 501.00m l = 501.00m
5⅛″ (142.9mm)	504.00m ~ 1002.75m	4½″ STO J-55	200m ~ 10000.00m l = 998.00m
HQ-WL (101.0mm)	1002.75m ~ 1227.34m	Open hole	

Fig. 3.2-5 Casing Program of GTE-7

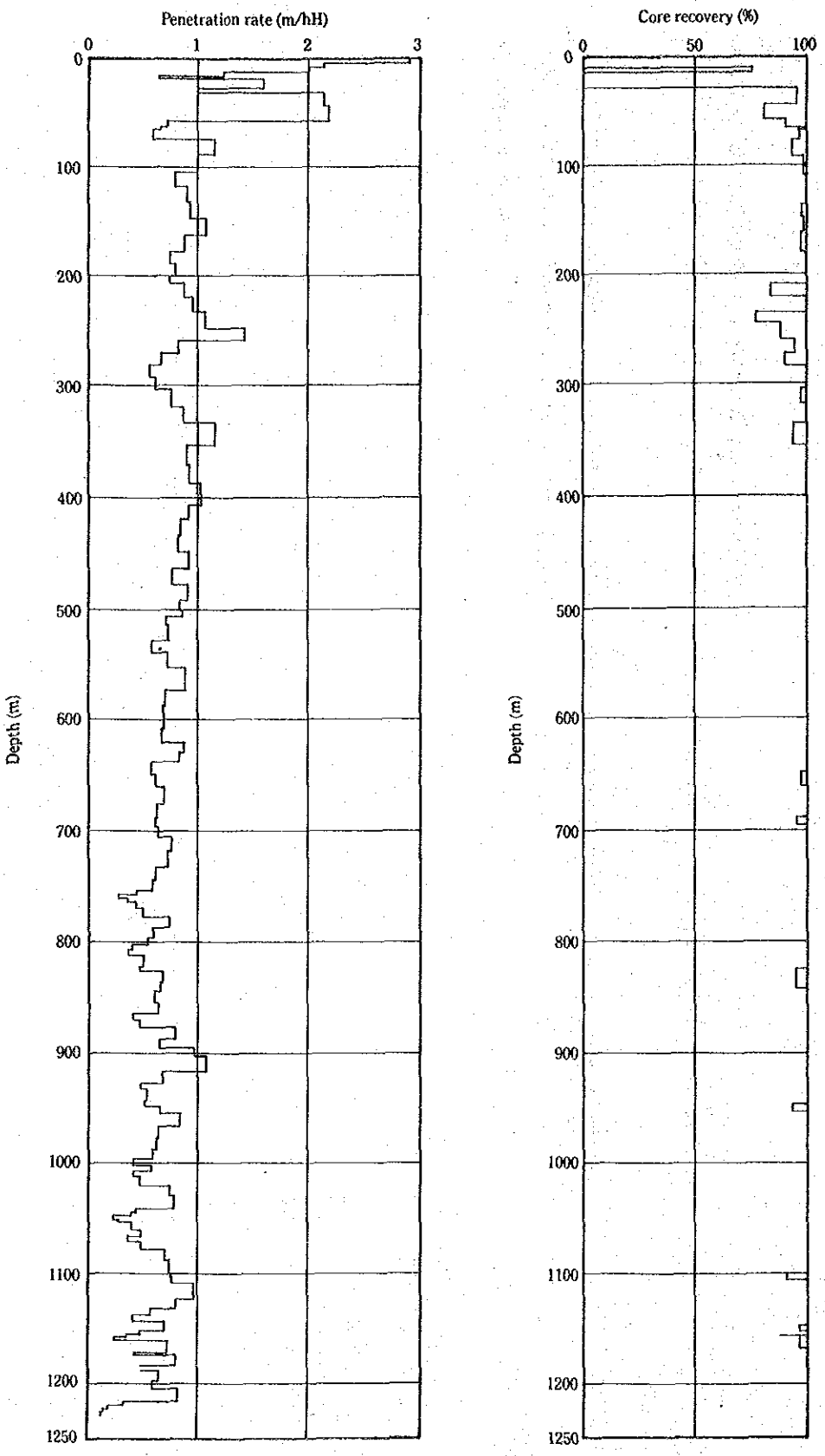

Fig. 3.2-6 Penetration Rate and Core Recovery of GTE-7

Depth (m)	Geological Column	Inclination	Rock Name	Rock Facies	Alteration	Number of Cracks (per meter) 15 10 5	Location of Sample: Depth (m)	M	X	D	Mg	P	T	F
10														
13.14							13.50		O					
20														
30		Non Core												
			sandstone	grey medium grained wacke (sandstone) with thin layer of black shale			32.50	O		O	O		O	O
		55					34.50	O	O					
		55					34.97							
40		60	shale	black black carbonaceous shale with arkosic sandstone (thin layer)	weathered									
		70												
50		67	(sandstone)		weathered									
		60	(sandstone)											
			(sandstone)				58.70		O					
60		55	siltstone	grey grey alternation of siltstone, sandstone, black shale			63.00	O	O	O	O	O	O	
							70.04							
70							70.30	O	O	O	O	O	O	
			shale	black carbonaceous black shale			72.30		O					O
80							82.50		O					
90			sandstone	grey arkosic wacke medium grained contains shale fragments	pyrite calcite									
94.80			sandstone											
		60					97.00	O	O	O	O	O	O	
100														
108.5			shale				106.50	O	O	O	O	O	O	
110		70												
114.5														
120		70	sandstone	grey medium to fine arkosic wacke			118.30							O
130		60	shale and sandstone alteration	black grey sandstone (fine to medium) with black grey carbonaceous shale			128.50		O					
		50												
140		65												
		80												
		40					146.80	O	O	O	O	O	O	
150			shale	dark green sheared zone (149.70 ~ 153.90) brecciated and black clay quartz vein			154.00		O					O
			shale and siltstone	grey										
			limestone	black										
160			shale and siltstone alternation	grey	qz druse 160.50 clay		160.50		O					
163.8		65	limestone	grey										
170		70					173.00	O	O	O	O	O	O	O
		80												
180		40	mudstone, siltstone	greyish green mudstone ~siltstone			179.00	O	O	O	O	O	O	O
		60		reddish mudstone										
		60												
190			shale and siltstone alternation	black black shale and greenish siltstone alternated										
		65					199.00							O
200			shale											
		55	sandstone and shale alternation	grey grey siliceous medium grained sandstone and black shale										
210		60	shale with snadstone	black carbonaceous shale with thin layer of grey siliceous fine to medium sandstone										
		10					217.00	O	O	O	O	O	O	
220														
		70												
230														
240		50	chert and black shale alternation	black										
		30												
250														

M — Microscopic Observation
X — X-Ray Analysis
D — Density Test
Mg — Magnetism Test
P — P-wave Velocity Measurement
T — Heat Conductivity Measurement
F — Fluid Inclusion Test

sandstone
shale
siltstone
chent
limestone
tuff
fault breccia
quartz vein
bedding

Depth: 0m ~250m

Fig. 3.3-1 Compiled Column of GTE-7 (1)

Depth (m)	Geological Column	Inclination	Rock Name	Rock Facies	Alteration	Number of Cracks (per meter) 15 10 5	Location of Sample: Depth (m)	M	X	D	Mg	P	T	F
260		85	chert	dark grey: dark grey chert with black thin layer shale			263.50	○	○	○	○	○	○	
		85												
270		85		strong sheared (270.20 ~ 273.30) (Core loss)			273.00		○					
280			limestone, shale	black			280.00	○	○	○	○	○	○	
		60	limestone, shale	black										
290		60	limestone, limestone and shale	grey: muddy shale, grey to black										
		70	shale	black: carbonaceous shale			293.50							○
300		70	limestone	black: black limestone with intercalated black thin shale	calcite vein		301.50	○	○	○	○	○	○	
		75	shale and limestone alternation	limestone > black carbonaceous shale										
310		60	limestone	grey										
320		80					318.00	○	○	○	○	○	○	
330		80	limestone and black shale alternation	black carbonaceous shale > and limestone alternation										
		80												
340		60	brecciated black shale, shale	black			339.00		○					
		50					348.00	○	○	○	○	○	○	
350		40	sandstone	grey: arkosic wacke, medium grained										
		20	shale with thin layer of sandstone and siltstone	black: carbonaceous black shale and chert grey charty sandstone and siltstone alternation										
360		80												
370		85												
		80					375.00	○	○	○	○	○	○	
380		70			quartz vein 381.9 ~382.3		379.40		○					
		50					383.00							○
		50												
390		60												
		70												
		60												
		90												
400		80	chert	light grey			402.00	○	○	○	○	○	○	
		85	shale and chert alternation	carbonaceous shale and dark grey ~ light grey chert alternation										
410		85												
		65												
420		80												
		70												
430		80	shale and chert alternation	black: carbonaceous shale and dark grey chert alternation			430.30	○	○	○	○	○	○	
		60	limestone											
440		30	shale											
		85												
		70												
450		50	shale	black										
		70	silicified shale	breccinted (453.0 ~ 457.0) silicified by quartz vein	quartz vein 15 cm		455.00		○					○
460		60	shale	black: carbonaceous shale			465.00	○	○	○	○	○	○	
		60												
470		70												
		60	shale and siltstone alternation	black grey: black carbonaceous shale and grey siltstone alternation										
480		80												
		60		quartz veinlet network										
490		70					496.00	○	○	○	○	○	○	
500		70												

M — Microscopic Observation
X — X-Ray Analysis
D — Density Test
Mg — Magnetism Test
P — P-wave Velocity Measurement
T — Heat Conductivity Measurement
F — Fluid Inclusion Test

sandstone
shale
siltstone
chent
limestone
tuff
fault breccia
quartz vein
bedding

Depth: 250m ~500m

Fig. 3.3-2 Compiled Column of GTE-7 (2)